DETERMINATION OF FIELD IONIZATION SENSITIVITY COEFFICIENTS AND CHARACTERIZATION OF PETROLEUM SATURATE FRACTIONS BY MASS SPECTROMETRY

By

MICHELE RAE DERRICK

Bachelor of Science

Central State University

Edmond, Oklahoma

1977

Submitted to the Faculty of the Graduate College
of the Oklahoma State University
in partial fulfillment of the requirements
for the Degree of
MASTER OF SCIENCE
December, 1979

DETERMINATION OF FIELD IONIZATION SENSITIVITY COEFFICIENTS AND CHARACTERIZATION OF PETROLEUM SATURATE FRACTIONS BY MASS SPECTROMETRY

Thesis Approved:

Stuart Scheppele
Thesis Advisor

J Paul Devlin

Horacio Amorbola

Norman N Durham
Dean of Graduate College

ACKNOWLEDGMENTS

The author wishes to express her appreciation to her major adviser, Dr. S. E. Scheppele, for his guidance and assistance throughout this study. Gratitude is also expressed to the other committee members, Dr. H. A. Mottola, and Dr. J. P. Devlin for their valued assistance in preparation of the final manuscript.

Special appreciation is expressed to Drs. Q. Grindstaff and C. S. Hwang for their invaluable assistance and time spent on the experimental and technical aspects of this study. Grateful thanks are given to Janice Grindstaff for her help in typing the manuscript draft and to Janet Sallee for her expertise in typing the final copy.

With love and sincerity the author wishes to thank her parents for the devotion, encouragement and sacrifices given to the furtherment of her education. Loving gratitude is expressed to John for moral support and spiritual refurbishment.

TABLE OF CONTENTS

LIST OF TABLES

LIST OF FIGURES

NOMENCLATURE

s_m	mole sensitivity
s_g	gram sensitivity
S_m	relative mole sensitivity
S_g	relative gram sensitivity
N	number of moles
I_m	molecular ion intensity
α	ionization probability
β	supply velocity
γ	ratio of the parent to total ion intensity
H	hydrogen atom
F	field strength
W	tungsten
Φ	work function of metal
Pm	proton electron potential
Pw	image potential
I	ionization potential - eV
Z	effective nuclear charge/e
D	tunneling probability
U_o	potential difference between anode and cathode - V
R	distance between anode and cathode - cm
r_o	radius of curvature of emitter tip - cm^2
C	$(1 - 7.6 \times 10^{-4} Z^{1/2} F^{1/2} / I)^{1/2}$ - unitless

(cont.)

n_o	number of particles
A_o	emitter area - cm^2
P	pressure
m	mass of the particle
k	Boltzman constant
T	temperature - 573^oK
V	potential energy of the particle
μ	average dipole moment - debye
α	mean polarizability - $\mathring{A}^3$
σ	effective cross section of emitter
l	length of emitter - cm
RCS	relative cross section
RSF	relative sensitivity function
g_m	grams of the lightest isotopic molecule
MW_o	molecular weight of the lightest isotopic molecule
$P_{i,j}$	fractional percent natural abundance of the ith heavy isotope of the jth element
RA_m	relative abundance of the lightest isotopic molecule
C'	C x 6.8 x 10^7 as defined by I, F and C
$N(C)_i$	number of carbons in the ith compound
Δ/C	change in relative mole sensitivity per carbon number
b	orthogonal semi-axes and principle polarizability
$\mathring{A}$	angstrom

CHAPTER I

INTRODUCTION

Since the first investigation into the phenomena of field ionization (FI), it has become a widely used technique in mass spectrometry (1,2,3). The main advantage of the FI method as applied to the mass spectrometric analysis of complex mixtures results from the fact that the mass spectra of the components consist virtually of only molecular ions (4). With this simplified spectra, qualitative analysis of complicated organic mixtures such as crude-oil fractions is simplified using field-ionization mass spectrometry. However, quantitative analysis of the FI mass spectral data may be obtained from a mixture of unknown composition only if sufficient sensitivity coefficient data for the field ionization of each of the mixture's components are available. The purpose of this study is to determine a possible method for the prediction of field-ionization sensitivity coefficients and then to quantitatively analyze crude-oil fractions.

Experimentally, sensitivity coefficients of compounds in a standard mixture may be determined by using weights (moles) and ion intensities obtained from its mass spectra (5). For a mixture of A and B, the mole sensitivity of A, $s_m(A)$, and B, $s_m(B)$ are given by equations 1 and 2, respectively,

$$s_m(A) = \frac{I_m(A)}{N_A} \qquad (1)$$

$$s_m(B) = \frac{I_m(B)}{N_B} \tag{2}$$

in terms of the intensity of only the molecular ion resulting from the field ionization of the most abundant isotopic molecules of the given components, $I_m(A)$ and $I_m(B)$, and of the moles of A and B, N_A and N_B, in the mixture. Equations 1 and 2 were combined to obtain the mole sensitivity of B relative to A in equation 3. The gram sensitivity of

$$S_m(B) = \frac{s_m(B)}{s_m(A)} = \frac{I_m(B)\ N_A}{I_m(A)\ N_B} \tag{3}$$

of component B relative to component A, $S_g(B)$, is given by equation 4, in which M_A and M_B are the molecular weights of components A and B.

$$S_g(B) = \frac{S_m(B)\ M_A}{M_B} \tag{4}$$

Alternatively, equation 5 expresses $S_g(B)$ in terms of the number of grams of A and B, g_A and g_B, respectively.

$$S_g(B) = \frac{I_m(B)\ g_A}{I_m(A)\ g_B} \tag{5}$$

Theoretically, sensitivity coefficients have been considered by Beckey (6) to be a function of

1) the probability of field ionization (tunneling effect),
2) diffusion over the emitter surface (supply velocity),
3) stability of the molecular ions with respect to fragmentation provided all other instrumental and experimental factors are constant.

Thus, the sensitivity coefficient may be expressed as the product of these three factors as shown in equation 6

$$s_m(i) = f(\alpha)\ g(\beta)\ h(\gamma) \tag{6}$$

where α = ionization probability

β = supply velocity

γ = ratio of the parent to total ion intensity

An indepth examination of each of the parameter affecting the measured peak height, i.e. sensitivity, of a component in a mixture will lead to a better understanding of the field ionization phenomena and a possible method of prediction of field-ionization sensitivities.

CHAPTER II

FACTORS DETERMINING THE FIELD IONIZATION SENSITIVITY FUNCTION

Ionization Probability

The theory of the phenomena of field ionization for a hydrogen atom (H) may be represented by means of a potential diagram shown in Figure 1a (7). The broken curves show a one-dimensional cut through the Coulomb potential seen by the atom's electron in the absence of an external field. A field (F), parallel to the plane of the paper, deforms the potential, as shown by the solid lines, so that the electron sees a barrier of finite height and width. If this barrier is small enough, autoionization will occur. As shown in Figure 1b, the presence of a metal surface,such as Tungsten (W), with work function Φ, decreases the size of the barrier confronting the electron more than it is in free space for fields of equal strength. In the deformed Coulomb potential, i.e. the proton electron potential (Pm) and image potential (Pw), of a molecule, the ionization potential (I) is the difference between the external potential (F) and the effectively filled highest electron level (Φ) of the metal. The distance required for this deformation is given along the x-axis in Angstroms. At this certain minimum distance of the atom from the surface of the metal, the valence electron of the atom is raised to the Fermi level by the external field. The potential

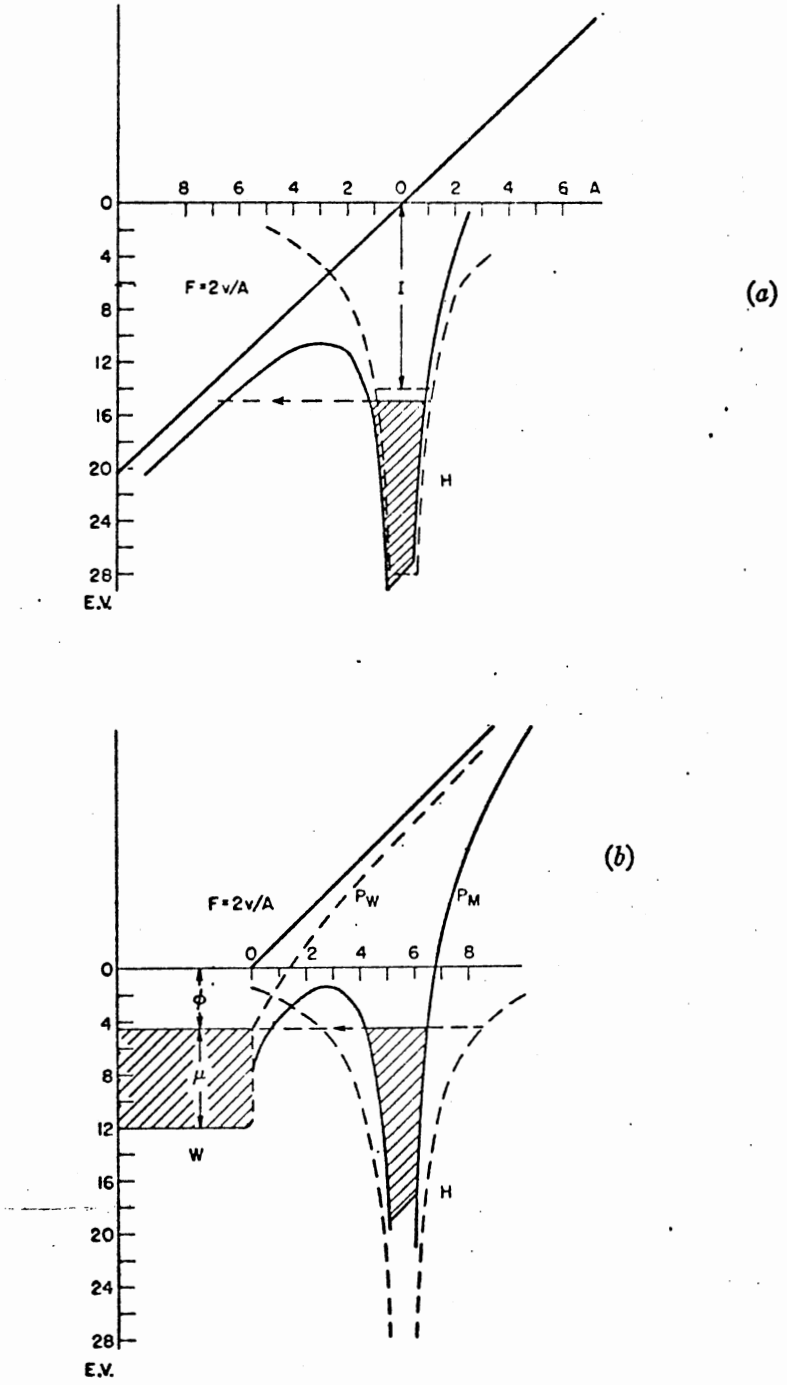

Figure 1. Diagrams Showing Proposed Mechanism for Field Ionization. (a) Potential-Energy Diagram for a Hydrogen Atom With and Without an External Field Present. (b) Ionization of Same Atom When it is Physically Adsorbed on a Tungsten Surface

barrier between the atom and the metal surface then has a width of only a few angstroms and a height of a few electron volts. Therefore, there exists a certain finite probability for the penetration of the electron through this barrier due to the quantum mechanical tunneling effect. The penetration coefficient or tunneling probability (D) has been calculated by Gomer (8) to be,

$$D = \exp\{-6.8 \times 10^{7}(I^{3/2}/F)\ (1 - 7.6 \times 10^{-4}\ Z^{1/2}\ F^{1/2}\ /I)^{1/2}\} \qquad (7)$$

where Z is the effective nuclear charge/e, I is the ionization potential in electron volts, and F is the field strength in volts per centimeter.

Equation 8 gives the field strength found at the surface of a sharp edge emitter of radius of curvature r_o for a potential difference

$$F_o = \frac{U_o}{r_o\sqrt{2}}\ \frac{1}{\sqrt{R/r_o}} \qquad (8)$$

U_o between it and the cathode at a distance R (9,10). The field ionization spectra were acquired in our laboratory at a field potential of 5800 $\pm$ 800 V. The anode is cut from Personna stainless steel razor blades. For these emitters, a reasonable estimate of r_o is 1×10^{-6}cm (9). A typical value of the anode/cathode distance R is .013 cm (11). These values lead to a field strength of ca. 3.6×10^{7} V/cm.

The term, $(1 - 7.6 \times 10^{-4}\ Z^{1/2}\ F^{1/2}\ /I)^{1/2}$, from equation 7 represents a corrective value for the image effect. Using exemplificative values, it may be illustrated as in Table I, that this term is essentially a constant with respect to the magnitude of the other terms in the equation. This constant (C) was taken to be 0.68.

Thus the tunneling probability (D) may be expressed as equation 9.

TABLE I

VARIATION OF IMAGE EFFECT CORRECTION WITH IONIZATION POTENTIAL[a]

I(ev)	C
10.0	0.74
9.8	0.73
9.6	0.72
9.4	0.72
9.2	0.71
9.0	0.70
8.8	0.69
8.6	0.69
8.4	0.68
8.2	0.67
8.0	0.66
7.8	0.64
7.6	0.63

[a] $C = (1 - 7.6 \times 10^{-4} Z^{1/2} F^{1/2} / I)^{1/2}$

for $Z = 1$ and $F = 3.6 \times 10^{7}$

$$D \simeq \exp\{-6.8 \times 10^7 \; I^{3/2} \; C/F\} \tag{9}$$

The tunneling probability for compound B relative to compound A is

$$\frac{D_B}{D_A} \simeq \frac{\exp\{-6.8 \times 10^7 \; I_B^{3/2} \; C/F\}}{\exp\{-6.8 \times 10^7 \; I_A^{3/2} \; C/F\}} \tag{10}$$

which may be further reduced

$$\frac{D_B}{D_A} \simeq \exp\{-6.8 \times 10^7 \; C/F \; (I_B^{3/2} - I_A^{3/2})\} \tag{11}$$

From equation 11, it is apparent that the relative tunneling probability is proportional to the exponential of the difference between the ionization potentials. Values for the ionization potentials of appropriate hydrocarbons were obtained from the literature (12,13,14).

Supply Velocity

The mechanism of current generation at a field emitter is a complex function of field and temperature (15). At sufficiently high fields, all particles approaching the tip are ionized before reaching it, so that the current is determined only be the supply function. As was pointed out by Muller (2), this exceeds the gas-kinetic value because molecules passing near the tip are attracted to it by polarization forces.

The number of particles approaching the ionization zone, i.e. the supply function, varies with field strength. At zero field strength, the number of particles, n_o, approaching the emitter area, A_o, is

$$n_o = A_o \cdot P \; (2\pi mkT)^{-1/2} \tag{12}$$

where P is the pressure, m is the mass of the particle, k is the Boltzman constant, and T is the temperature (8).

In the presence of a field, the potential energy V of a particle may be expressed in terms of its average dipole moment in the direction of the field (μ) and its polarizability (α) as shown in equation 13 (4).

$$-V(F) = \mu F + 1/2\ \alpha F^2 \tag{13}$$

Equation 14 reveals that the effective cross section of the emitter (A) for the capture of gas particles is increased by the electric field (4).

$$\frac{A}{A_o} = \sigma = 1 - \frac{2/3\ V(F_o)}{kT} \tag{14}$$

The cross section for particle supply may be approximated by $A_o = 2\pi r^2 l$, where l is the length of the emitter. The effective cross section in the presence of a field would then be, $A = 2\pi r^2 l \cdot \sigma$. Thus the supply function for particles in a field becomes

$$n = 2\pi r^2 l \sigma\ P(2\pi mkT)^{-1/2}. \tag{15}$$

The relative supply function for compound B with respect to compound A is denoted as

$$\frac{n(B)}{n(A)} = \frac{2\pi r^2 l \sigma_B P(2\pi m_B kT)^{-1/2}}{2\pi r^2 l \sigma_A P(2\pi m_A kT)^{-1/2}} \tag{16}$$

Since compounds A and B are two constituents of a mixture, the experimental conditions may be assumed to be equivalent for each one. Thus, equation 16 reduces to

$$\frac{n(B)}{n(A)} = \frac{\sigma_B (m_B)^{-1/2}}{\sigma_A (m_A)^{-1/2}} \tag{17}$$

Substitution of the relationship $\sigma = 1 - 2/3\ \frac{\mu F + 1/2\ \alpha F^2}{kT}$ into equation 17 leads to equation 18.

$$\frac{n(B)}{n(A)} = \frac{kT - 2/3(\mu_B F + 1/2\alpha_B F^2)\ m_A^{1/2}}{kT - 2/3(\mu_A F + 1/2\alpha_A F^2)\ m_B^{1/2}} \tag{18}$$

Thus the supply function of any compound relative to the supply function of the reference compound is functionally dependent on the masses, the average permanent dipole moments, and the polarizabilities of both components. Obviously, values for the molecular weight of any compound are easily obtainable. Literature values for the permanent dipole moments of the compounds of interest are available (15,16). In the present calculations, the dipole moment is negligible compared to the polarizability for the field strengths employed. This is demonstrated for some compounds in Table II. Polarizability values obtained as described in Appendix A were used in determining the relative sensitivity functions.

Experimental Estimates of Relative Cross Sections for Field Ionization

It should be noted that the relative cross section for field ionization is the quantity which should be correlated with the ionization probability and supply function. For each component in a mixture, the intensity of the isotopically-most-abundant molecular ion divided by the number of moles of this species is proportional to the cross section for field ionization.

Since for the compounds studied, the molecular ions accounted for greater than 95% of the singly-charged ions, fragmentation was considered negligible.

Assuming other instrumental and experimental factors to be the same, the relative field ionization cross sections, RCS(FI), may be calculated as a function of structure and mixture composition using the intensity of the isotopically most abundant molecular ion of each component in the mixture, which, in the case of the compounds studied,

TABLE II

COMPARISON OF THE DIPOLE MOMENTS AND POLARIZABILITY FACTORS AS FOUND IN EQUATION 18 FOR VARIOUS HYDROCARBONS

Compound	Dipole Moments μ (debyes)	$\mu F(eV)^a$	$\frac{1}{2}\alpha F^2(eV)^a$
N-Paraffins	0.00	0.00	~0.20
Benzene	0.00	0.00	0.09
Toluene	0.43	9.0×10^{-6}	0.11
Ethylbenzene	0.37	7.7×10^{-6}	0.13
1,2-Dimethylbenzene	0.45	9.4×10^{-6}	0.13
1,3-Dimethylbenzene	0.30	6.2×10^{-6}	0.13
1,4-Dimethylbenzene	0.00	0.00	0.13
Propylbenzene	0.35	7.3×10^{-6}	0.15

[a] $F = 3.6 \times 10^7$ V/cm

corresponds to the lightest isotopic ions. The calculations must also use both the grams and the molecular weight of the lightest isotopic molecule for each component in the mixture, g_m and MW_o, respectively.

$$RCS(B) = \frac{I_m(B) \;/\; g_m(B) \;/\; MW_o(B)}{I_m(A) \;/\; g_m(A) \;/\; MW_o(A)} \tag{19}$$

Consider a compound with a molecular formula $C_{x1}H_{x2}N_{x3}O_{x4}S_{x5}$ in which x_j is the number of atoms of the jth element in the compound. The molecular weight for the lightest isotopic molecule may easily be calculated by the summation of the exact masses for each of the lightest isotopic atoms contained in the molecule. The weight, g_m of the lightest isotopic molecule may be calculated by equation 20,

$$g_m = \frac{g_t}{1 + \frac{g_{m+1}}{g_M} + \cdots \frac{g_{m+n}}{g_m}} \tag{20}$$

where g_{m+n} is the weight of the molecule having n heavy isotopic molecules. The ratio of g_{m+n} to g_m is the summation of the combinations of the fractional percent natural abundances, $P_{i,j}$ and $P_{o,j}$, of the ith heavy isotope to the lightest isotope of the jth element as given in equation 21

$$\frac{g_{m+n}}{g_m} = \sum_{i=1}^{n} \sum_{j=1}^{5} X_j \frac{P_{i,j} MW_{i,j}}{P_{o,j}} \frac{1}{MW_o}^n \tag{21}$$

$MW_{i,j}$ is the molecular weight of the compound containing the ith heavy isotope of the jth element.

Previously, equation 20 was used for the calculation of the weight of the lightest isotopic molecule with the expansion in equation 21 carried out to n=2 (18). The neglect of molecules containing three or more heavy isotopes results in an error which increases with molecular

weight, as demonstrated in Table III. This error tends to be negligible with respect to the experimental errors of the run.

In order to not induce any unnecessary error into the calculations of the relative cross section, a second method has been utilized for the determination of the weight of the lightest isotopic molecule. The ratio of the weight of the lightest isotopic molecules to the total weight of all molecules is in essence the relative abundance of the lightest isotopic molecule (RA_m) to the total molecules. Using the relative abundance for the lightest isotope of each atom, (i.e. $C_{12} = 0.98888$, $H_1 = 0.999855$, $N_{14} = 0.99633$, $O_{16} = 0.99759$, and $S_{32} = 0.95018$, for the compound $C_{x_1}H_{x_2}N_{x_3}O_{x_4}S_{x_5}$ in which x_j is the number of atoms of the jth element) the relative abundance for the lightest isotopic molecule may be represented by equation 23.

$$\frac{g_m}{g_t} = RA_m \tag{22}$$

$$RA_m = (RA_C)^{x_1}(RA_H)^{x_2}(RA_N)^{x_3}(RA_O)^{x_4}(RA_S)^{x_5} \tag{23}$$

Now that the fractional abundance of the lightest isotopic molecule has been determined, we may substitute equation 22 into equation 19, producing equation 24.

$$RCS(B) = \frac{I_m(B)/g_T(B) \cdot RA_{m(B)}/\dot{MW}_o(B)}{I_m(A)/g_T(A) \cdot RA_{m(A)}/MW_o(A)} \tag{24}$$

Thus the relative cross section in terms of the relative mole sensitivity is as follows:

$$RCS(B) = S_m(B) \times \frac{RA_{m(A)}}{RA_{m(B)}} \tag{25}$$

Using this method, values for the FI relative cross section for

TABLE III

ERROR INDUCED BY THE NEGLECTION OF THE CONTRIBUTIONS OF MORE THAN TWO HEAVY ISOTOPES FOR n-PARAFFINS

Carbon Number	Molecular Weight	Percent of Total Weight[a]
5	72.09	100.00
10	142.17	99.98
15	212.25	99.94
20	282.33	99.85
25	352.41	99.71
30	422.49	99.52
35	492.56	99.26
40	562.64	98.92
45	632.72	98.52
50	702.80	98.04

[a] $\frac{g_m + g_{m+1} + g_{m+2}}{g_T} \times 100$

several hydrocarbons have been calculated from experimental sensitivity coefficients and are given in Table IV.

Now, in terms easily obtainable, the relative mole sensitivity has been corrected for the ratio of the parent ion intensity to the total ion intensity for the field ionization of a compound.

TABLE IV

RELATIVE CROSS SECTIONS FOR VARIOUS HYDROCARBONS

Compound	Molecular Weight	Relative[a] FI Mole Sensitivities	Relative[a] FI Cross Sections
Hexane	86.11	0.59	0.56
Heptane	100.12	0.90	0.87
Octane	114.14	0.81	0.79
Nonane	128.16	0.93	0.91
Decane	142.17	1.00	1.00
Undecane	156.19	1.07	1.08
Dodecane	170.20	1.22	1.25
Tridecane	184.22	1.35	1.40
Tetradecane	198.23	1.44	1.51
Pentadecane	212.25	1.53	1.62
Hexadecane	226.27	1.64	1.76
Heptadecane	240.28	1.67	1.81
Octadecane	254.30	1.78	1.95
Nonadecane	268.31	1.91	2.12
Eicosane	282.33	1.92	2.16
Heneicosane	296.34	2.08	2.38
Docosane	310.36	2.00	2.31
Tetracosane	338.39	2.38	2.80
Benzene	78.05	0.90	0.88
Toluene	92.06	1.02	1.01
Ethylbenzene	106.08	1.00	1.00
1,2-Dimethylbenzene	106.08	1.10	1.10
1,3-Dimethylbenzene	106.08	1.09	1.09
1,4-Dimethylbenzene	106.08	1.11	1.11
Propylbenzene	120.09	1.02	1.03
1,3,5-Trimethylbenzene	120.09	1.14	1.15
Naphthalene	128.06	1.25	1.28
Methylnaphthalene	142.08	1.27	1.31
1,6-Dimethylnaphthalene	156.09	1.44	1.51
2,3-Dimethylnaphthalene	156.09	1.55	1.62
Fluorene	166.08	1.44	1.52
Phenanthrene	178.08	1.63	1.74
Anthracene	178.08	1.78	1.90
Pyrene	202.08	1.56	1.70
Fluoranthene	202.08	1.69	1.85

[a]Mole Sensitivity and Cross Section 1) for Saturates are relative to decane and 2) for Aromatics are relative to ethylbenzene.

CHAPTER III

PROPORTIONALITY CORRELATION

If the sensitivity coefficients per unit of compound charged are dependent on the field-ionization probability, the supply velocity to the emitter suface, and the ratio of the parent ion to the total ion intensity, then it must hold true that the relative cross section for any component is directly proportional to a function of the relative tunneling probability,

$$\frac{D(B)}{D(A)} = \exp\left\{-\frac{C'}{F}\left(I_B^{3/2} - I_A^{3/2}\right)\right\} \tag{26}$$

where $C' = C \times 7.6 \times 10^7$

and the relative supply function,

$$\frac{n(B)}{n(A)} = \frac{\{kT - 2/3(\mu_B F + 1/2\alpha_B F^2)\}\, m_A^{1/2}}{\{kT - 2/3(\mu_A F + 1/2\alpha_A F^2)\}\, m_B^{1/2}} \tag{27}$$

A combination of these terms in the form of compound B relative to compound A will be defined as the sensitivity function and is given by equation 28.

$$RCS(B) \propto \frac{\{kT - 2/3(\mu_B F + 1/2\alpha_B F^2)\}\, m_A^{1/2}}{\{kT - 2/3(\mu_A F + 1/2\alpha_A F^2)\}\, m_B^{1/2}} \exp\left\{\frac{-C'}{F}\left(I_B^{3/2} - I_A^{3/2}\right)\right\} \tag{28}$$

Calculated values for these terms for several saturate and aromatic hydrocarbons are given in Table V and Table VI, respectively. Plots for the experimental FI relative cross sections versus the rela-

TABLE V

RELATIVE SENSITIVITY FUNCTIONS FOR SATURATE HYDROCARBONS

Compound	Molecular Weight	Polarizability (A^3)	Ionization Potential (eV)	Relative Sensitivity Function[a]
Hexane	86.11	11.5	10.17	0.66
Heptane	100.12	13.3	10.06	0.76
Octane	114.14	15.1	10.03	0.85
Nonane	128.16	16.9	10.02	0.93
Decane	142.17	18.7	9.95	1.00
Undecane	156.19	20.5	9.93	1.07
Dodecane	170.20	22.3	9.93	1.14
Tridecane	184.22	24.0	9.92	1.19
Tetradecane	198.23	25.8	9.92	1.25
Pentadecane	212.25	27.6	9.91	1.31
Hexadecane	226.27	29.4	9.91	1.37
Heptadecane	240.28	31.2	9.9	1.43
Octadecane	254.30	33.0	9.9	1.48
Nonadecane	268.31	34.8	9.9	1.53
Elcosane	282.33	36.6	9.9	1.58
Heneicosane	296.34	38.4	9.9	1.63
Docosane	310.36	40.2	9.9	1.68
Tetracosane	338.39	43.7	9.9	1.76

[a]Relative to Decane

TABLE VI

RELATIVE SENSITIVITY FUNCTIONS FOR AROMATIC HYDROCARBONS

Compound	Molecular Weight	Polarizability ($Å^3$)	Ionization Potential (eV)	Relative Sensitivity Function[a]
Benzene	78.05	9.87	9.245	0.72
Toluene	92.06	11.7	9.20	0.87
Ethylbenzene	106.08	13.5	9.12	1.00
1,2-Dimethylbenzene	106.08	13.5	9.01	0.98
1,3-Dimethylbenzene	106.08	13.57	8.96	0.98
1,4-Dimethylbenzene	106.08	13.6	8.86	0.97
Propylbenzene	120.09	15.3	8.72	1.05
1,3,5-Trimethylbenzene	120.09	15.4	8.76	1.06
Naphthalene	128.06	16.5	8.12	1.02
Methylnaphthalene	142.08	18.1	7.96	1.06
2,6-Dimethylnaphthalene	156.09	19.8	7.77	1.09
1,3-Dimethylnaphthalene	156.09	19.8	7.85	1.11
Fluorene	166.08	20.1	7.78	1.08
Phenanthrene	178.08	23.6	8.03	1.34
Anthracene	178.08	23.6	7.43	1.19
Pyrene	202.08	28.2	7.53	1.41
Fluoranthene	202.08	28.8	7.72	1.50

[a] Relative to Ethylbenzene.

tive sensitivity function are shown in Figures 2, 3, and 4. Figure 2 represents the values for n-paraffins relative to decane, Figure 3 represents the values for aromatic type compounds relative to ethyl benzene and Figure 4 is a combination of both types of hydrocarbons. These figures show that a reasonable linear correlation exists between the relative cross sections for field ionization and the calculated relative sensitivity function for the hydrocarbons shown. A least squares function was used to fit lines to the points. The slope, intercept, and associated standard deviations for the least squares lines shown in Figures 2, 3, and 4 are listed in Table VII. Thus, the least squares parameters given in Table VII for the hydrocarbon values may be used to predict relative cross section values for any hydrocarbon for which the sensitivity function may be calculated. Table VIII lists the relative cross section values which have been obtained experimentally and those which have been calculated using the parameters obtained by the least squared fit of the data in Figure 4 using equation 29

$$RCS_i = 1.76(RSF_i) - .60 \qquad (29)$$

where RSF_i stands for the relative sensitivity function for the ith component. The relative difference for the predicted values and the experimental values is also given in Table VIII. In the majority of cases, this error falls within the uncertainty calculated from the error in the experimental relative mole sensitivities.

Thus, the relative sensitivity function provides reasonable approximations to the experimentally determined field ionization relative cross sections. This function may be used to obtain estimate values for field ionization sensitivity coefficients which have not previously been experimentally determined.

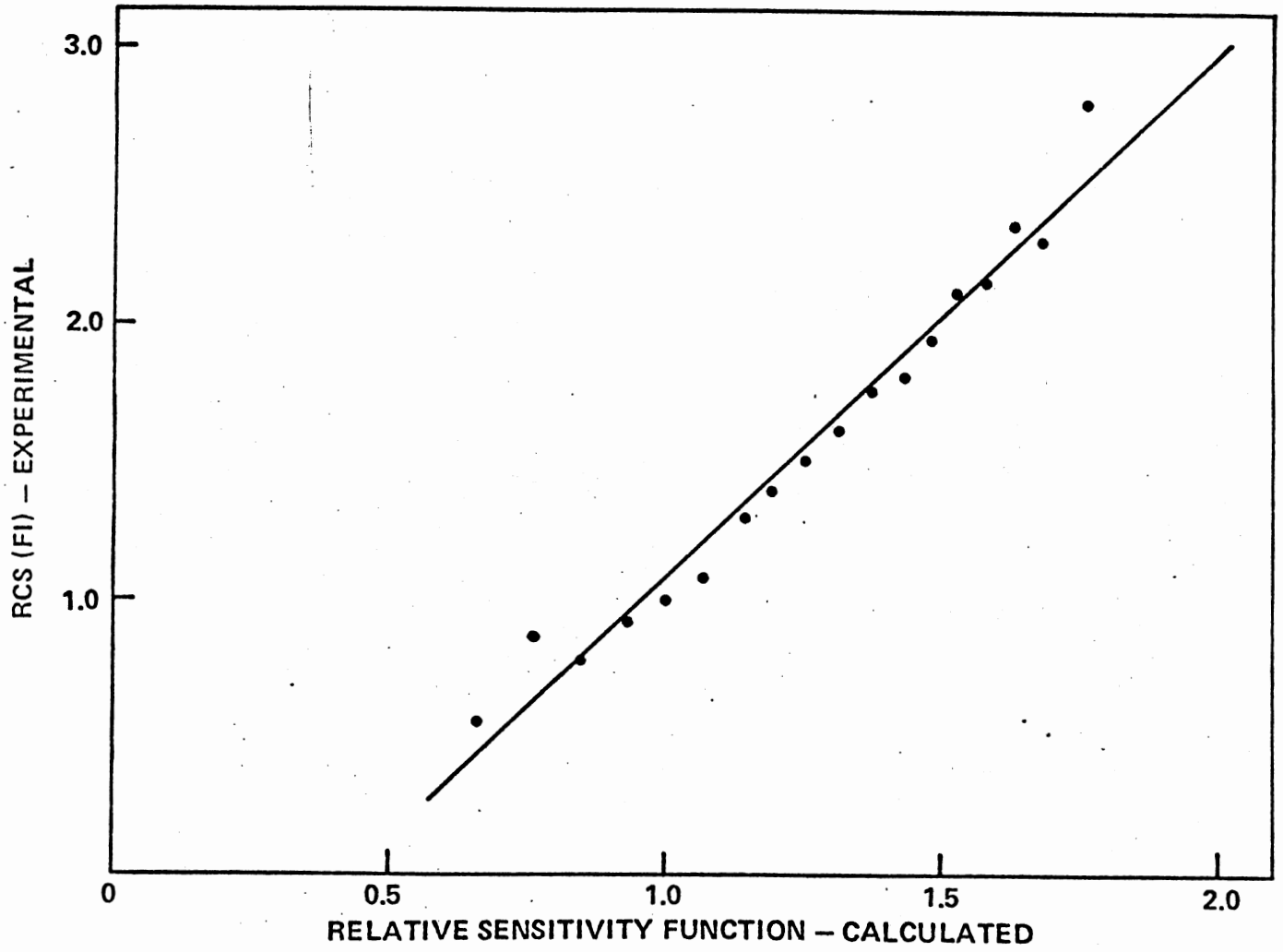

Figure 2. Plot of Relative Cross Section Versus Relative Sensitivity Function for n-Paraffin Hydrocarbons

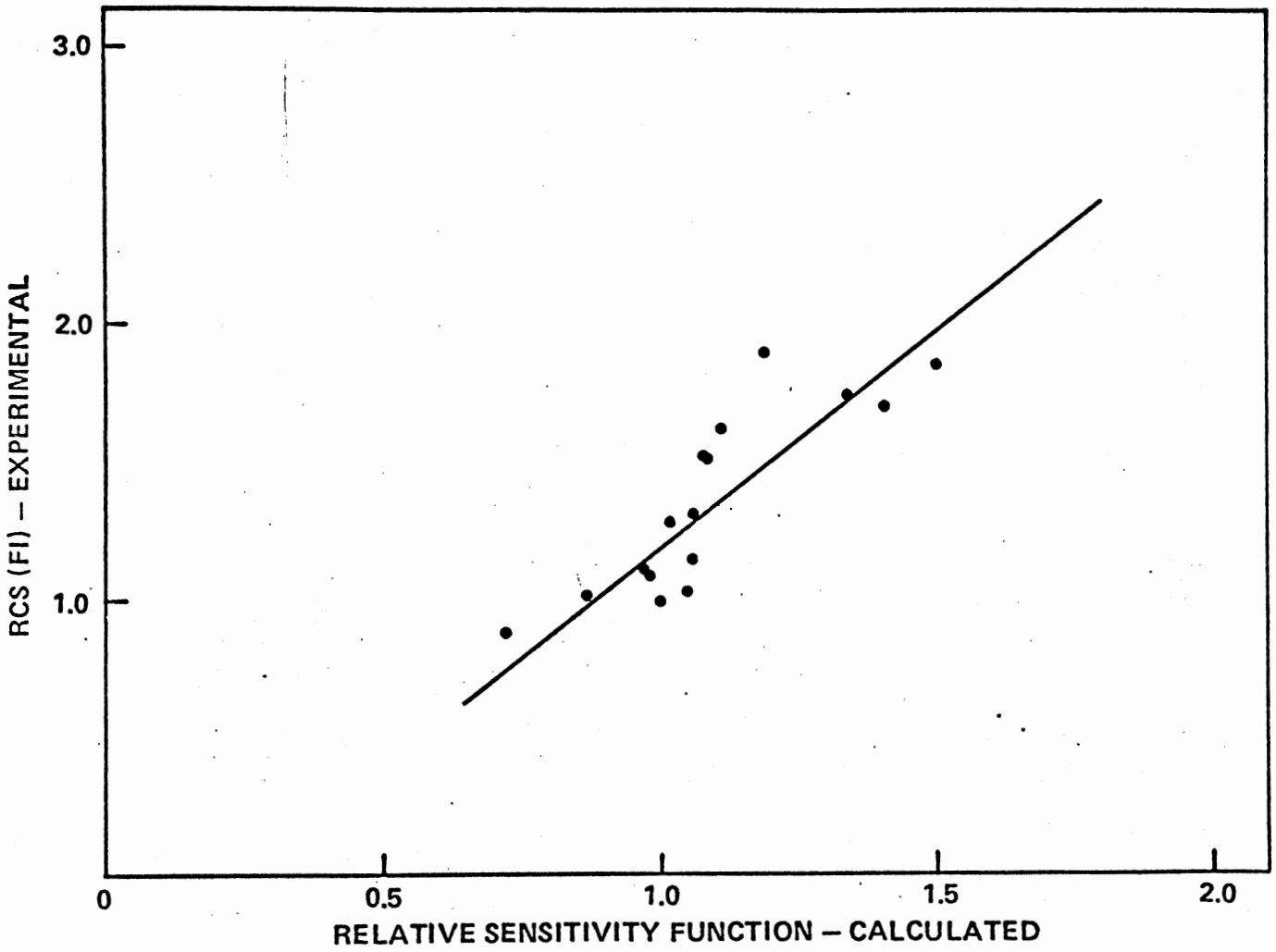

Figure 3. Plot of Relative Cross Section Versus Relative Sensitivity Function for Aromatic Hydrocarbons

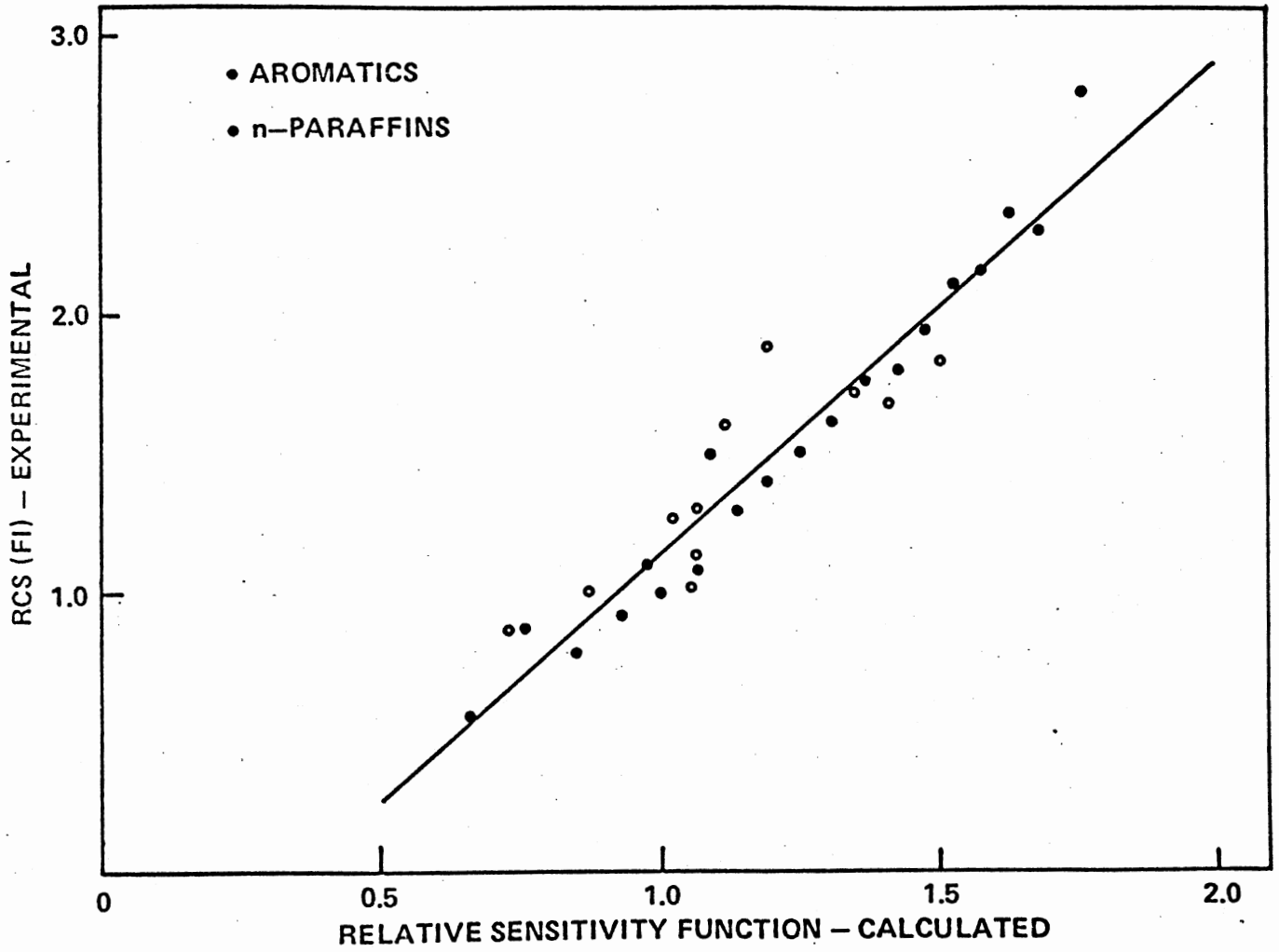

Figure 4. Plot of Relative Cross Section Versus Relative Sensitivity Function for n-Paraffins and Aromatice Hydrocarbons

TABLE VII

CORRELATION CONSTANTS FOR THE FI RELATIVE CROSS SECTIONS WITH THE RELATIVE SENSITIVITY FUNCTIONS

Compound Type	Slope	Intercept
N-Paraffin Hydrocarbons	1.91 ± .11	-0.83 ± .12
Aromatic Hydrocarbons	1.48 ± .16	-0.26 ± .17
Both types of Hydrocarbons	1.76 ± .14	-0.60 ± .14

TABLE VIII

RELATIVE CROSS SECTIONS PREDICTED FROM THE SENSITIVITY FACTOR AS COMPARED TO EXPERIMENTAL RCS(FI)

Compound	Experimental RCS(FI)	Predicted RCS(FI)	Relative Error
Hexane	0.56	0.56	0.00
Heptane	0.87	0.73	0.16
Octane	0.79	0.89	0.13
Nonane	0.92	1.03	0.12
Decane	1.00	1.16	0.16
Undecane	1.08	1.28	0.19
Dodecane	1.25	1.40	0.12
Tridecane	1.40	1.49	0.06
Tetradecane	1.51	1.59	0.05
Pentadecane	1.62	1.70	0.05
Hexadecane	1.76	1.81	0.03
Heptadecane	1.81	1.91	0.06
Octadecane	1.95	2.00	0.03
Nonadecane	2.12	2.09	0.01
Eicosane	2.16	2.17	0.01
Heneicosane	2.38	2.26	0.05
Docosane	2.31	2.35	0.02
Tetracosane	2.80	2.49	0.11
Benzene	0.88	0.66	0.25
Toluene	1.01	0.93	0.08
Ethylbenzene	1.00	1.16	0.16
1,2-Dimethylbenzene	1.10	1.12	0.02
1,3-Dimethylbenzene	1.09	1.12	0.03
1,4-Dimethylbenzene	1.11	1.10	0.01
Propylbenzene	1.03	1.24	0.21
1,3,5-Trimethylbenzene	1.15	1.26	0.10
Naphthalene	1.28	1.19	0.07
Methylnaphthalene	1.31	1.26	0.04
1,6-Dimethylnaphthalene	1.51	1.31	0.13
2,3-Dimethylnaphthalene	1.62	1.35	0.17
Fluorene	1.52	1.30	0.15
Phenanthrene	1.74	1.75	0.01
Anthracene	1.90	1.49	0.22
Pyrene	1.70	1.88	0.10
Fluoranthene	1.85	2.03	0.10

[a] $$\frac{RCS(FI)_E - RCS(FI)_P}{RCS(FI)_E} = RE$$

CHAPTER IV

EXPERIMENTAL DETERMINATION OF FIELD IONIZATION SENSITIVITY COEFFICIENTS

Instruments

Field ionization mass spectra were acquired using a CEC 21-110B double focusing mass spectrometer equipped with a modified combination FI/EI ion source. Spectra were obtained with an emitter (ion-accelerating potential) of 5.8 kV and a counter electrode potential of +800 to -800 V. Emitters were cut from an uncoated stainless-steel razor blade (Personna 74) and conditioned in the ion source at 300°C in the presence of acetone (ca. 2×10^{-5} Torr). The samples were introduced into the ion source via 1) an all-glass inlet system (320°C) and 2) a direct-introduction, temperature programmable probe. The mass spectra were obtained on an AEI DS-50S data acquisition system.

The interface between the data system and the mass spectrometer provides for simultaneous computer-controlled scanning of the magnetic field and acquisition of the analog signal from the electron multiplier as a function of time. A mass spectrum can thus be computer logged for operation of the mass spectrometer in the field ionization mode. Multiple scans of the mass spectrum can be acquired to improve the signal-to-noise ratio.

The gas chromatograms were obtained using a Perkin-Elmer 3920

equipped with a dual flame ionization detector (FID), a Leeds and Northrup 610 recorder, and a CSI Supergrator 3 programmable computing integrator. All separations utilized a 5% OV-101 on Gas Chrom Z AW-DMSC (100/120) glass column (12ft. x 1/8 in.).

Compounds

N-Paraffins in the carbon number range of 12-21 used in mixtures #1 and #2 were obtained from Aldrich Chemical and were listed as > 99% pure. Compounds used in the remaining mixtures were obtained from the Bartlesville Energy Research Center, from E. J. Eisenbraun's group at Oklahoma State University, and from commercial sources. The purity of each sample was established using 1) isothermal and temperature programmed FID/GC and 2) FI/MS with an ion source temperature of 270-300°C.

Standard mixtures were prepared using weighed quantities of each sample and then stored at 0°C. The composition of the majority of the mixtures were verified by GC analysis using temperature programming. The gas chromatograms indicated that any impurities present contributed negligibly.

Analysis and Results

The relative field ionization mole sensitivities for all the aromatic compounds and for the lower molecular weight n-paraffins (C_6-C_{13}, C_{16}, C_{18}, C_{19}) were previously published values (18,19). Thus, it was necessary to obtain relative sensitivities for higher molecular weight n-paraffins.

Three standard mixtures of n-paraffins were used for the direct analysis of the sensitivity coefficients. Two mixtures, MIX #1 and

MIX #2, were prepared at Oklahoma State University, and contained the following compounds: $C_{12}H_{26}$, $C_{13}H_{28}$, $C_{14}H_{30}$, $C_{15}H_{32}$, $C_{16}H_{34}$, $C_{17}H_{36}$, $C_{18}H_{38}$, $C_{19}H_{40}$, $C_{20}H_{42}$, and $C_{21}H_{44}$. The third mixture, MIX #3, which was prepared at the Bartlesville Energy Research Center, contained the following components: $C_{11}H_{24}$, $C_{12}H_{26}$, $C_{14}H_{30}$, $C_{15}H_{32}$, $C_{16}H_{34}$, $C_{19}H_{40}$, $C_{21}H_{44}$, $C_{22}H_{46}$, and $C_{24}H_{50}$. The verification of the weight percent composition of each of these mixtures was done by temperature programmed FID/GC. The results are given in Table IX. Three chromatographic runs were performed on each of the standard mixtures. Exemplitive chromatograms for standard mixtures #1, #2, and #3, are illustrated by Figures 5, 6, and 7, respectively.

The experimental determination of the field ionization sensitivity coefficients were made by two techniques. The first method consisted of introducing the sample into the ion source via and all-glass batch inlet system. Two injections were made for each sample with five computer scans taken for each injection. Mass/intensity reports for mixtures #1, #2, and #3 are shown by Figures 8, 9, and 10, respectively. The second method utilized for the experimental determination of the sensitivity coefficients was micromolecular probe distillation. This technique is described more thoroughly in Appendix B.

For each compound gram sensitivity coefficients were calculated relative to hexadecane. The results obtained for each mixture and for the probe distillation are given in Table X. The final average given for each component is an average of the sensitivity values determined for the component from each run performed on that component.

The previous field ionization relative mole sensitivity value for hexadecane relative to decane has been determined to be 1.64 (18).

TABLE IX

GAS CHROMATOGRAPHIC ANALYSIS OF STANDARD n-PARAFFIN MIXTURES

Compound	Actual Weight Percent			Weight Percent Determined by GC[a]		
	Mix #1	Mix #2	Mix #3	Mix #1	Mix #2	Mix #3
Undecane			12.63			12.00 ± .51
Dodecane	9.89	8.59	14.07	9.57 ± .24	8.94 ± .23	13.60 ± .55
Tridecane	10.39	9.85		10.46 ± .46	10.02 ± .24	
Tetradecane	10.14	8.05	13.71	10.35 ± .37	8.81 ± .05	12.90 ± .32
Pentadecane	9.79	10.87	11.29	10.06 ± .07	10.80 ± .13	11.77 ± .16
Hexadecane	10.21	9.96	11.12	10.31 ± .07	10.01 ± .16	11.33 ± .25
Heptadecane	8.95	9.93		9.26 ± .23	10.04 ± .14	
Octadecane	10.85	12.41		10.69 ± .19	11.39 ± .32	
Nonadecane	10.20	11.05	9.27	9.73 ± .46	10.69 ± .06	9.76 ± .14
Eicosane	9.66	12.50		9.87 ± .45	11.71 ± .31	
Heneicosane	9.91	6.80	10.27	9.59 ± .33	7.61 ± .31	9.92 ± .29
Docosane			9.30			9.45 ± .43
Tetracosane			8.35			9.19 ± .76

[a]Averages of three runs for each mixture.

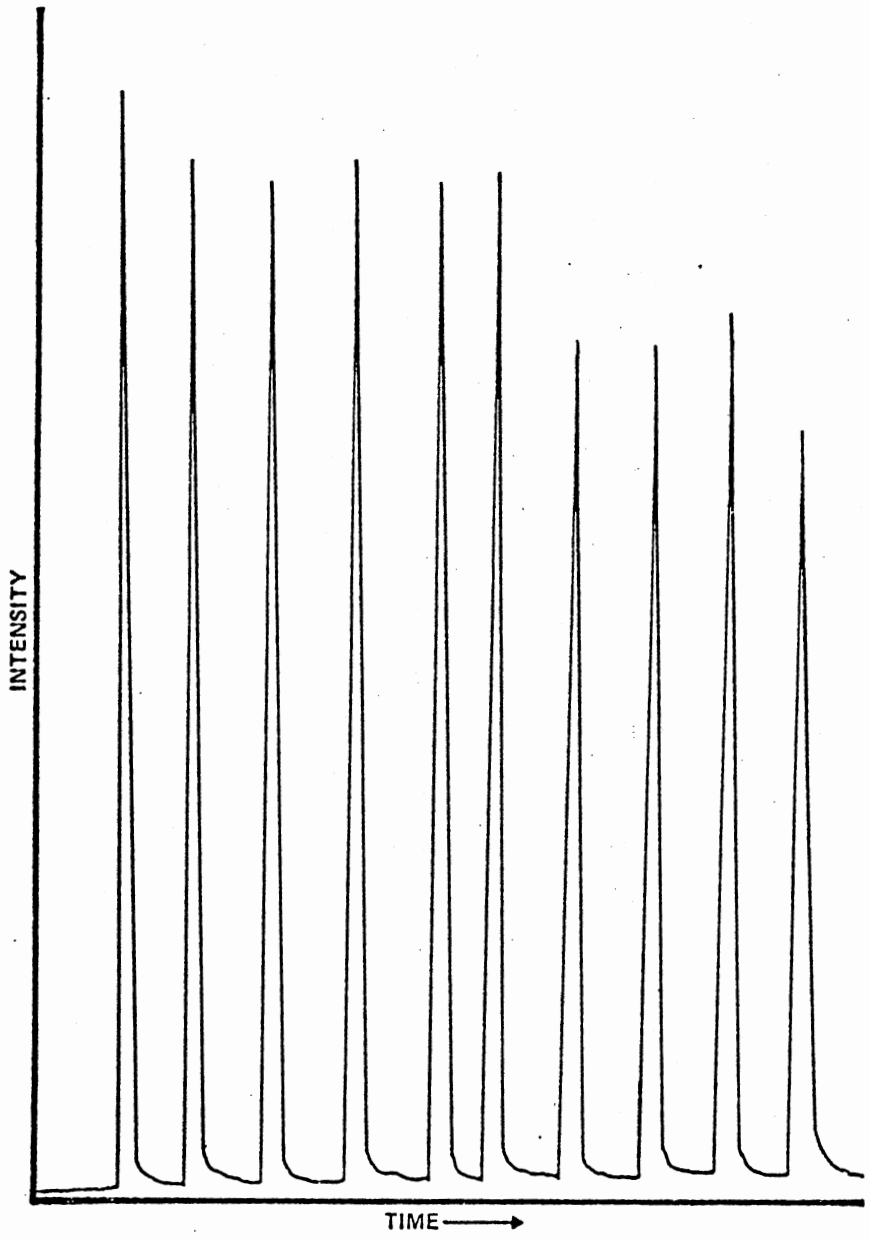

Figure 5. Gas Chromatogram of Standard Mixture #1. The Order of Elution Follows the Compounds Listed in Table IX in Descending Sequence

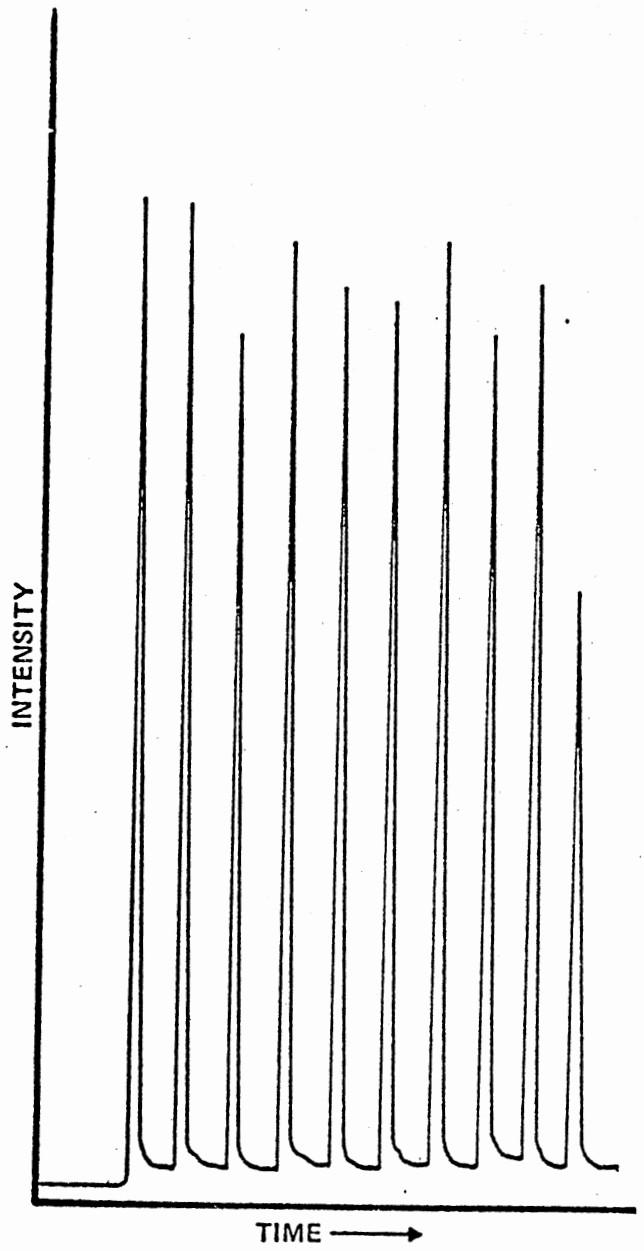

Figure 6. Gas Chromatogram of Standard Mixture #2. The Order of Elution Follows the Compounds Listed in Table IX in Descending Sequence

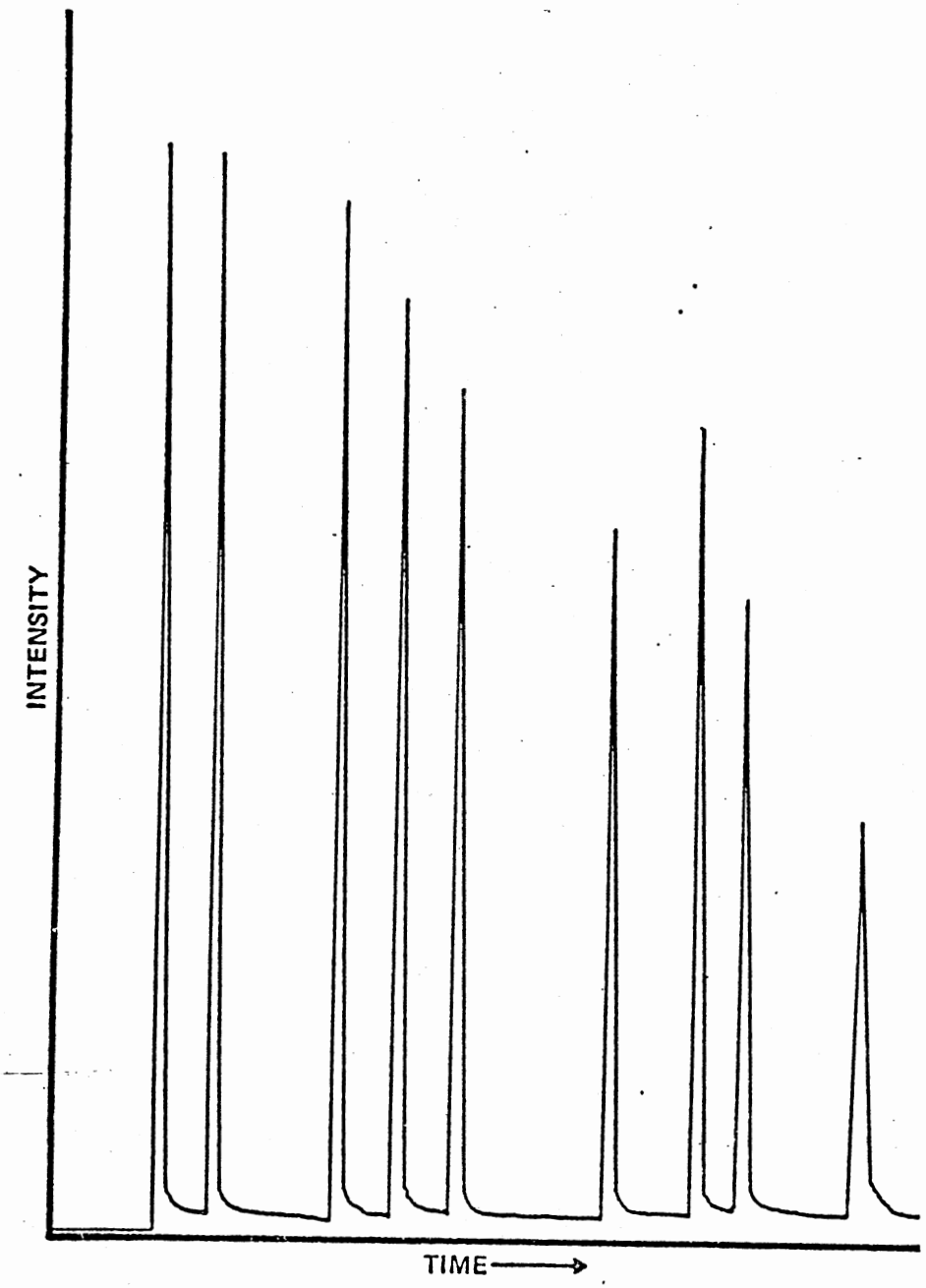

Figure 7. Gas Chromatogram of Standard Mixture #3. The Order of Elution Follows the Compounds Listed in Table IX in Descending Sequence

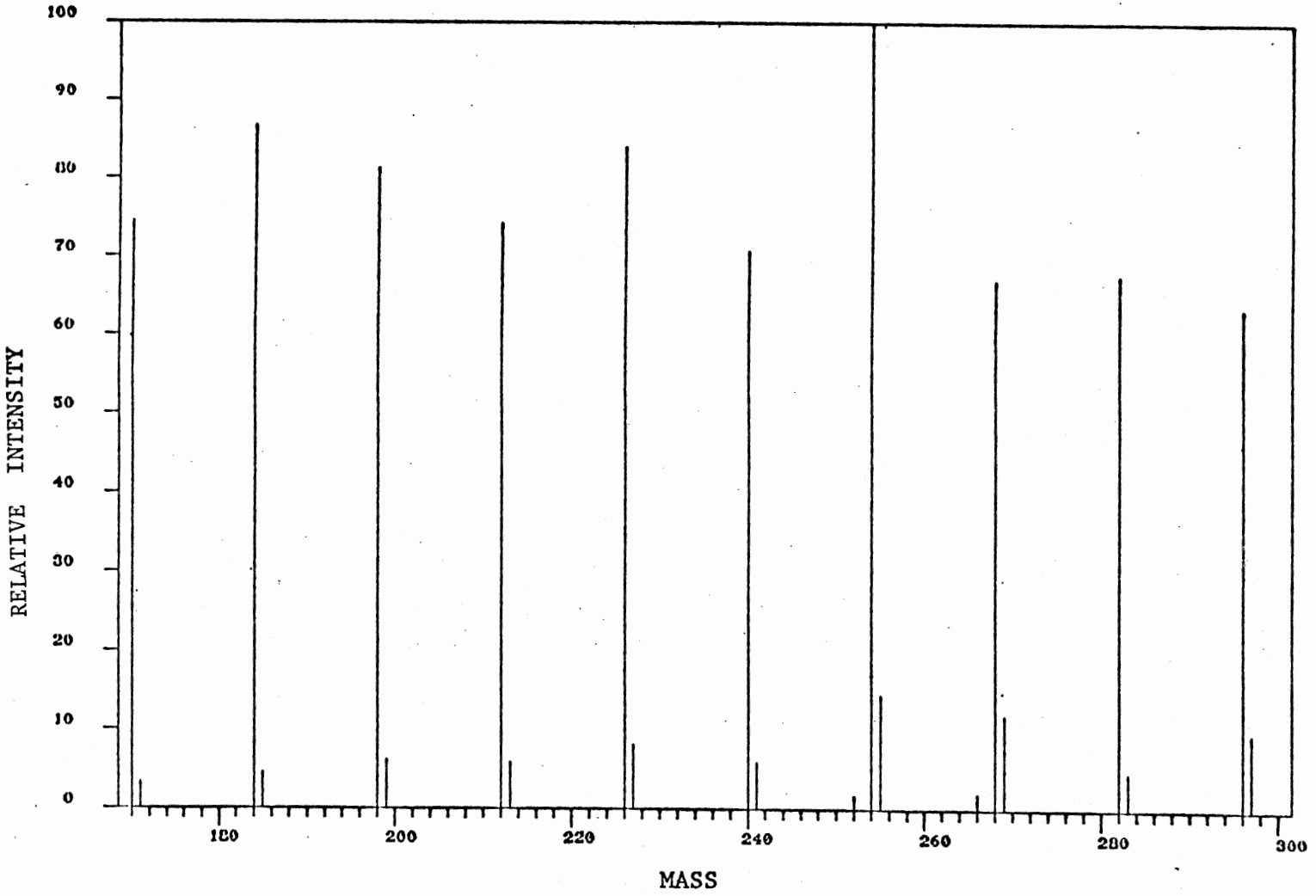

Figure 8. Field Ionization Mass Spectra of n-Paraffin MIX 1

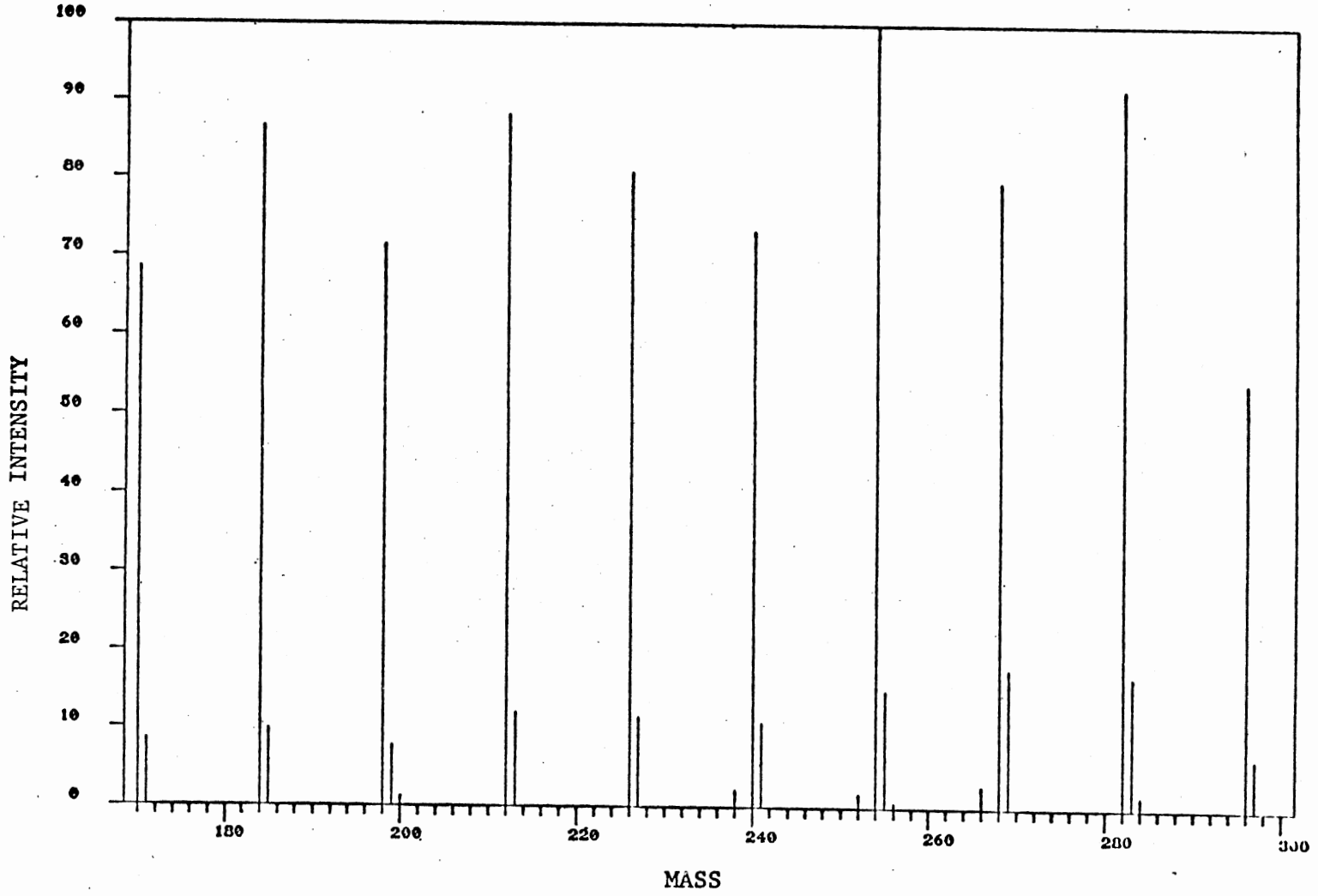

Figure 9. Field Ionization Mass Spectra of n-Paraffin MIX 2

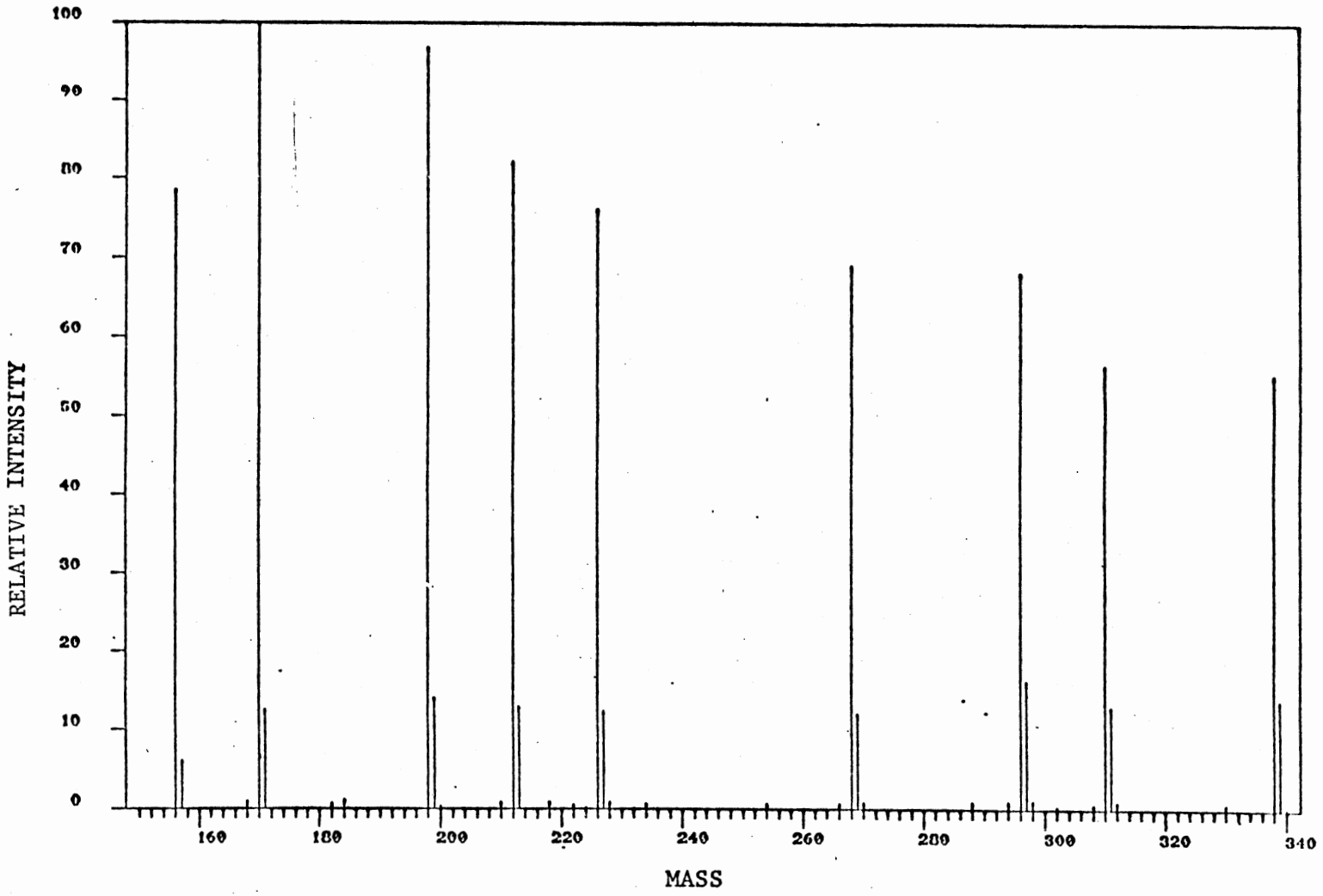

Figure 10. Field Ionization Mass Spectra of n-Paraffin MIX 3

TABLE X

EXPERIMENTALLY DETERMINED RELATIVE GRAM SENSITIVITY VALUES FOR n-PARAFFINS

Compound	Batch Inlet System			Probe Distillation	Average
	Mix#1	Mix#2	Mix#3	Mix#1	
Undecane			0.91±.10		0.91±.10
Dodecane	0.92±.01	0.92±.09	1.04±.06	1.33	1.01±.06
Tridecane	0.97±.07	1.00±.11		1.27	1.04±.09
Tetradecane	0.96±.01	1.05±.07	1.03±.04	1.05	1.02±.05
Pentadecane	0.95±.04	1.01±.01	1.06±.07	1.05	1.01±.06
Hexadecane	1.00	1.00	1.00	1.00	1.00
Heptadecane	0.95±.01	0.98±.09		1.19	1.01±.06
Octadecane	1.06±.09	1.02±.04		1.06	1.04±.06
Nonadecane	0.90±.13	0.95±.08	1.09±.11	1.06	0.99±.11
Eicosane	0.91±.08	0.96±.11		1.11	0.98±.09
Heneicosane	0.90±.16	1.00±.01	1.07±.09	1.02	0.99±.10
Docosane			0.89±.13		0.89±.13
Tetracosane			0.97±.05		0.97±.05

[a]Relative to Hexadecane

Using this value, the sensitivities relative to hexadecane obtained from mixtures #1, #2, and #3 were converted to the use of decane as a reference compound. This is shown in Table XI. Relative mole sensitivities for dodecane, tridecane, octadecane, and nonadecane were previously determined to be 1.19, 1.31, 1.73, and 1.92, respectively (18). For Table IV, the past and present determinations of sensitivity coefficients were averaged for these compounds.

Recently, a fourth mixture was run by field ionization mass spectrometry in order to determine the senstivity coefficients of n-paraffins at a higher molecular weight. This mixture contained: $C_{19}H_{40}$, $C_{20}H_{42}$, $C_{21}H_{44}$, $C_{22}H_{46}$, $C_{23}H_{48}$, $C_{25}H_{52}$, $C_{26}H_{54}$, $C_{28}H_{58}$, $C_{30}H_{62}$, and $C_{34}H_{70}$. From the results of one determination, Table XII gives the 1) relative gram senstivities for each component relative to Eicosane, 2) relative cross sections for each constituent relative to Eicosane, 3) relative cross section for each compound relative to Decane using the previously determined value of Eicosane as a conversion factor, and 4) the predicted values of the relative cross sections using equation 29. The agreement between the new experimental values and the predicted is still within the limits of acceptability. Thus, the correlation still holds true for these compounds.

TABLE XI

RELATIVE SENSITIVITIES WITH HEXADECANE AND DECANE AS REFERENCE COMPOUNDS

Compound	Relative to Hexadecane		Relative to Decane	
	S_g	S_m	S_m	RCS
Undecane	0.91	0.63	1.03	1.04
Dodecane	1.01	0.76	1.25	1.28
Tridecane	1.04	0.85	1.39	1.44
Tetradecane	1.02	0.89	1.46	1.53
Pentadecane	1.01	0.95	1.56	1.65
Hexadecane	1.00	1.00	1.64	1.76
Heptadecane	1.01	1.07	1.75	1.90
Octadecane	1.04	1.17	1.92	2.11
Nonadecane	0.99	1.17	1.92	2.13
Eicosane	0.99	1.24	2.03	2.28
Heneicosane	0.99	1.30	2.13	2.42
Docosane	0.89	1.22	2.00	2.31
Tetracosane	0.97	1.45	2.38	2.80

TABLE XII

EXPERIMENTAL AND PREDICTED SENSITIVITIES
FOR n-PARAFFINS FROM MIX #4

Compound	$\frac{s(g)_i}{s(g)_{C_{20}}}$	$\frac{RCS_i}{RCS_{C_{20}}}$	$\frac{RCS_i}{RCS_{C10}}$	Predicted RCS
Nonadecane	0.90	0.88	1.83	2.09
Eicosane	1.00	1.00	2.16	2.17
Heneicosane	0.99	1.00	2.08	2.26
Docosane	0.82	0.94	1.96	2.35
Tricosane	0.81	0.97	2.02	2.42
Pentacosane	0.89	1.15	2.39	2.57
Hexacosane	0.88	1.19	2.48	2.64
Octacosane	1.08	1.57	3.27	2.78
Triacontane	0.90	1.41	2.93	2.92
Tetratriacontane	0.92	1.63	3.39	3.20

CHAPTER V

QUANTITATIVE ANALYSIS OF SATURATED HYDROCARBON FRACTIONS OF PETROLEUM CRUDES

The identification and quantification of fossil-energy materials are of biological and environmental concern. Presently, the combination of mass spectrometry with computer technology provides rapid and routine acquisition of information concerning the identity and amounts of compound types present in a sample. Characterizations of crude oil types may then be made and applied to oil spill studies, geochemical studies, and crude oil pricing criteria.

For this study, field ionization mass spectra, FI/MS, were acquired in order to obtain a qualitative and quantitative analysis of petroleum saturate fractions numbered: 71011, 72054, 73065, 75046, 75052 fraction 1, 75052 fraction 2, 75064, 76064, and 78001. These saturated hydrocarbon fractions were produced by separation of the original crude oils using an alumina-silica column at the Bartlesville Energy Technology Center. In order to insure the removal of all aromatic constituents, the eluents from the column were monitored continuously using a sensitive UV detector.

In principle, field ionization can be developed as a technique for obtaining molecular-ion group-type characterization of these saturated fractions. Such an analysis provides the weight percent of the homolog as a function of hydrocarbon type. The accuracy of the distribution re-

flects the dependance of the FI sensitivity coefficients on saturate structure. As shown in Chapter IV, the relative gram sensitivities for FI of the n-alkanes are essentially independent of the number of carbon atoms in the n-alkanes. Assuming this trend may be applied to all saturated hydrocarbon series, it would be necessary only to determine the relative gram sensitivity for the first member of the saturated-hydrocarbon-type series in order to calculate compositional data. Prediction of the relative gram sensitivities of the first member of a saturated-hydrocarbon-type series have been made by Scheppele et al. (18) by using the following equation,

$$\frac{s(g)_i}{s(g)_R} = \frac{(MW)_R\{(\Delta/C_i)[N(C)_i - N(C)_R] + 1\}}{14\ N(C)_i + Z} \tag{30}$$

where $s(g)_i$ and $s(g)_R$ are the gram sensitivities for the ith and reference compounds, respectively, MW_R is the molecular weight of the reference compound, $N(C)_i$ and $N(C)_R$ are the number of carbons in the ith and reference compounds respectively, and Δ/C_i is the change in the relative mole sensitivity per carbon number which may be calculated by

$$\frac{\Delta}{C_i} = \frac{s(m)_i/s(m)_R - 1}{N(C)_i - N(C)_R} \quad . \tag{31}$$

The values of the relative gram sensitivities used in the present analysis are given in Table XIII.

Using these values for the relative gram sensitivities within an homologous z-series, the weight percents for any compound may be determined by equation 32, where $s(g)_i$ and $s(g)_j$ are the relative gram

$$(wt\%)_i = \frac{I_j/s(g)_i}{\sum_{i=1}^{N} (I_i/s(g)_i)} \times 100 \tag{32}$$

TABLE XIII

RELATIVE GRAM SENSITIVITY VALUES FOR SATURATE HYDROCARBON TYPE SERIES

Z Series	First Member of Series	$\frac{s(g)_i}{s(g)_R}$
+2	$C_{10}H_{22}$	1.00
0	C_6H_{12}	2.2
-2	$C_{10}H_{18}$	4.1
-4	$C_{13}H_{22}$	5.2
-6	$C_{16}H_{26}$	5.5
-8	$C_{19}H_{30}$	5.8
-10	$C_{22}H_{34}$	6.1

sensitivities for the ith and jth components and I_i and I_j are their corresponding ion intensities.

In Tables XIV through XXII each petroleum saturate fraction has been characterized by weight percents and carbon number distributions for each of the hydrocarbon-type series present in the sample. The average carbon number for each series is a weighted mean. The weighted mean is calulated by summing the product of the carbon number and its weight percent for each homolog in each z-series.

Mass/Intensity plots for each of the samples are illustrated by Figures 11-19. The weight percent and carbon number distributions may also be performed inclusive of the total sample data set. Results of the type of analysis are given in Table XXIII.

For the majority of the samples, two runs were performed. The agreement in the characterization of these two runs for samples #71011, #75046, #75064, and #78001 fall within an acceptable 10% deviation. For the remaining fractions, it is apparent that a minimum of one more run should be performed on each sample before any definite conclusions may be drawn as to their characteristics.

For each sample, an estimate of the percent fragmentation was determined by the summation of the ion intensities occuring at m/e 43, 57, 71, 85, and 99. In all cases, the percent fragmentation accounted for less than 7.3% of the total ion intensity of the sample. The average fragmentation for all runs was found to be 2.7%. For the purposes of this study, the fragmentation was assumed negligible and no corrections were attempted.

A high resolution scan was taken for each of the petroleum saturate fractions. In each of the scans, the only doublet found to be prevalent

TABLE XIV

CHARACTERIZATION OF PETROLEUM #71011 SATURATE FRACTION THROUGH QUANTITATIVE Z-SERIES ANALYSIS OF TWO MASS SPECTROMETRIC RUNS

Z-Series	Weight Percents		Carbon Number Range					
			Run#1			Run#2		
	Run#1	Run#2	Initial	Final	Average	Initial	Final	Average
2	39.85	32.11	6	35	12.07	7	35	11.55
0	35.44	36.68	6	35	11.55	6	38	11.60
-2	15.57	19.07	8	40	14.17	8	41	13.96
-4	5.11	6.67	11	35	17.37	10	40	17.58
-6	3.05	3.88	14	37	23.10	13	39	22.32
-8	0.84	1.30	15	33	23.63	15	38	24.63
-10	0.14	0.30	18	26	23.44	18	35	23.56

TABLE XV

CHARACTERIZATION OF PETROLEUM #72054 SATURATE FRACTION THROUGH QUANTITATIVE Z-SERIES ANALYSIS OF TWO MASS SPECTROMETRIC RUNS

Z-Series	Weight Percents		Carbon Number Range					
			Run#1			Run#2		
	Run#1	Run#2	Initial	Final	Average	Initial	Final	Average
2	76.39	68.47	6	42	18.43	6	40	13.76
0	16.41	18.83	6	44	21.47	6	43	14.74
-2	4.04	6.93	9	46	22.39	8	43	16.25
-4	1.55	3.00	11	45	24.27	11	40	18.5
-6	0.87	1.56	14	46	26.94	13	41	22.31
-8	0.35	0.74	15	39	26.62	14	32	21.65
-10	0.38	0.48	17	40	28.08	17	33	23.53

TABLE XVI

CHARACTERIZATION OF PETROLEUM #73065 SATURATE FRACTION BY QUANTITATIVE Z-SERIES ANALYSIS

Z-Series	Weight Percents	Carbon Number Range		
		Initial	Final	Average
2	73.43	6	34	16.57
0	18.88	6	35	17.58
-2	5.24	12	36	21.07
-4	1.22	14	21	16.95
-6	1.23	19	30	24.59

TABLE XVII

CHARACTERIZATION OF PETROLEUM #75046 SATURATE FRACTION THROUGH QUANTITATIVE Z-SERIES ANALYSIS OF TWO MASS SPECTROMETRIC RUNS

Z-Series	Weight Percents		Carbon Number Range					
			Run#1			Run #2		
	Run#1	Run#2	Initial	Final	Average	Initial	Final	Average
2	46.33	40.51	6	31	10.70	6	34	10.77
0	38.70	38.35	6	34	10.51	6	36	10.78
-2	10.21	13.37	8	34	13.60	8	35	13.50
-4	2.87	3.99	11	37	18.48	10	34	17.41
-6	1.26	2.38	14	33	22.40	14	34	22.33
-8	0.55	1.00	18	33	25.49	16	38	25.08
-10	0.08	0.40	18	24	20.68	21	37	27.62

TABLE XVIII

CHARACTERIZATION OF PETROLEUM #75052 SATURATE FRACTION #1 THROUGH QUANTITATIVE Z-SERIES ANALYSIS OF TWO MASS SPECTROMETRIC RUNS

Z-Series	Weight Percents		Carbon Number Range					
			Run#1			Run#2		
	Run#1	Run#2	Initial	Final	Average	Initial	Final	Average
2	71.15	63.91	6	37	15.59	6	33	10.64
0	19.64	25.24	6	42	16.25	6	33	11.31
-2	5.00	6.92	9	41	17.66	8	35	14.24
-4	2.00	2.21	11	40	21.37	11	36	17.78
-6	1.64	1.20	15	38	26.91	14	35	21.92
-8	0.38	0.32	16	37	27.25	15	30	19.86
-10	0.18	0.21	17	31	23.30	18	26	21.12

TABLE XIX

CHARACTERIZATION OF PETROLEUM #75052 SATURATE FRACTION #2 THROUGH QUANTITATIVE Z-SERIES ANALYSIS OF TWO MASS SPECTROMETRIC RUNS

Z-Series	Weight Percents		Carbon Number Range					
			Run#1			Run#2		
	Run#1	Run#2	Initial	Final	Average	Initial	Final	Average
2	75.14	51.93	6	31	11.94	6	27	10.13
0	18.98	31.85	6	33	11.81	6	30	10.56
-2	3.91	10.77	9	33	15.55	7	30	12.90
-4	1.19	3.04	11	30	17.01	10	30	14.72
-6	0.68	1.49	14	30	24.12	13	32	19.44
-8	0.09	0.84	27	30	28.51	15	35	24.63
-10	0.00	0.07	--	--	--	19	22	20.37

TABLE XX

CHARACTERIZATION OF PETROLEUM #75064 SATURATE FRACTION THROUGH QUANTITATIVE Z-SERIES ANALYSIS OF TWO MASS SPECTROMETRIC RUNS

Z-Series	Weight Percents		Carbon Number Range					
			Run#1			Run#2		
	Run#1	Run#2	Initial	Final	Average	Initial	Final	Average
2	46.06	42.38	6	33	11.17	6	26	10.38
0	40.25	42.86	6	37	10.66	6	33	10.13
-2	10.28	12.66	8	37	13.17	8	36	12.22
-4	2.15	2.09	11	38	18.45	10	36	15.89
-6	0.89	0.68	14	34	22.39	12	32	19.61
-8	0.26	0.23	18	31	24.63	14	29	19.21
-10	0.11	0.10	19	31	23.49	17	28	20.29

TABLE XXI

CHARACTERIZATION OF PETROLEUM #76046 SATURATE FRACTION BY QUANTITATIVE Z-SERIES ANALYSIS

Z-Series	Weight Percents	Carbon Number Range		
		Initial	Final	Average
2	52.60	6	22	12.35
0	37.32	6	24	13.52
-2	8.17	9	25	14.67
-4	1.63	12	24	16.34
-6	0.17	15	17	16.16
-8	0.07	17	17	17.00
-10	0.04	19	19	19.00

TABLE XXII

CHARACTERIZATION OF PETROLEUM #78001 SATURATE FRACTION THROUGH QUANTITATIVE Z-SERIES ANALYSIS OF TWO MASS SPECTROMETRIC RUNS

Z-Series	Weight Percents		Carbon Number Range					
			Run#1			Run#2		
	Run#1	Run#2	Initial	Final	Average	Initial	Final	Average
2	68.87	62.28	6	29	9.84	6	25	9.89
0	24.91	28.76	6	38	10.22	6	34	10.34
-2	4.10	5.80	8	37	13.64	8	34	13.30
-4	1.38	1.82	11	31	16.82	10	31	15.23
-6	0.46	0.79	14	30	20.65	14	32	19.54
-8	0.25	0.40	15	29	20.73	15	31	20.36
-10	0.02	0.16	22	22	22.00	17	30	21.52

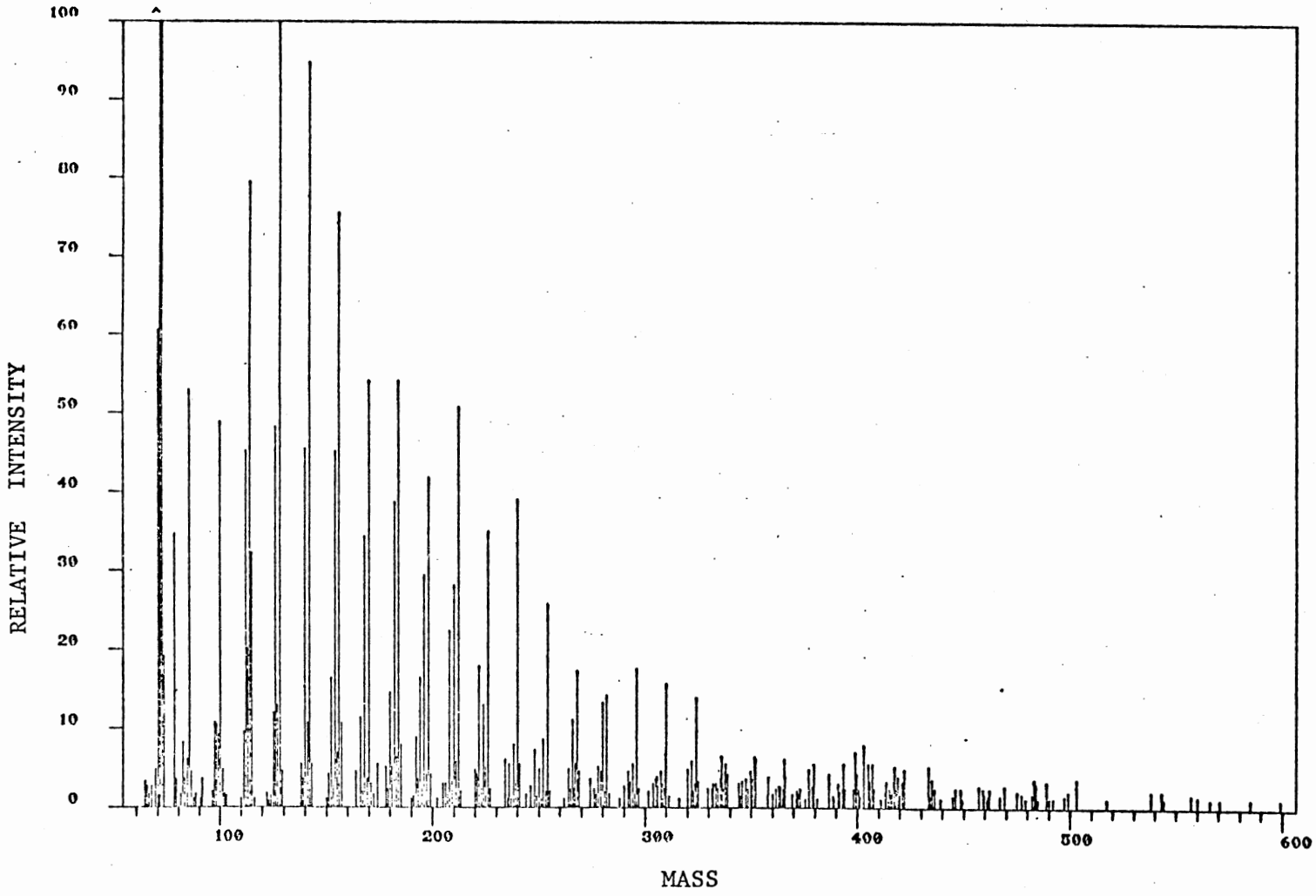

Figure 11. Field Ionization Mass Spectra of Petroleum Saturate Fraction 71011

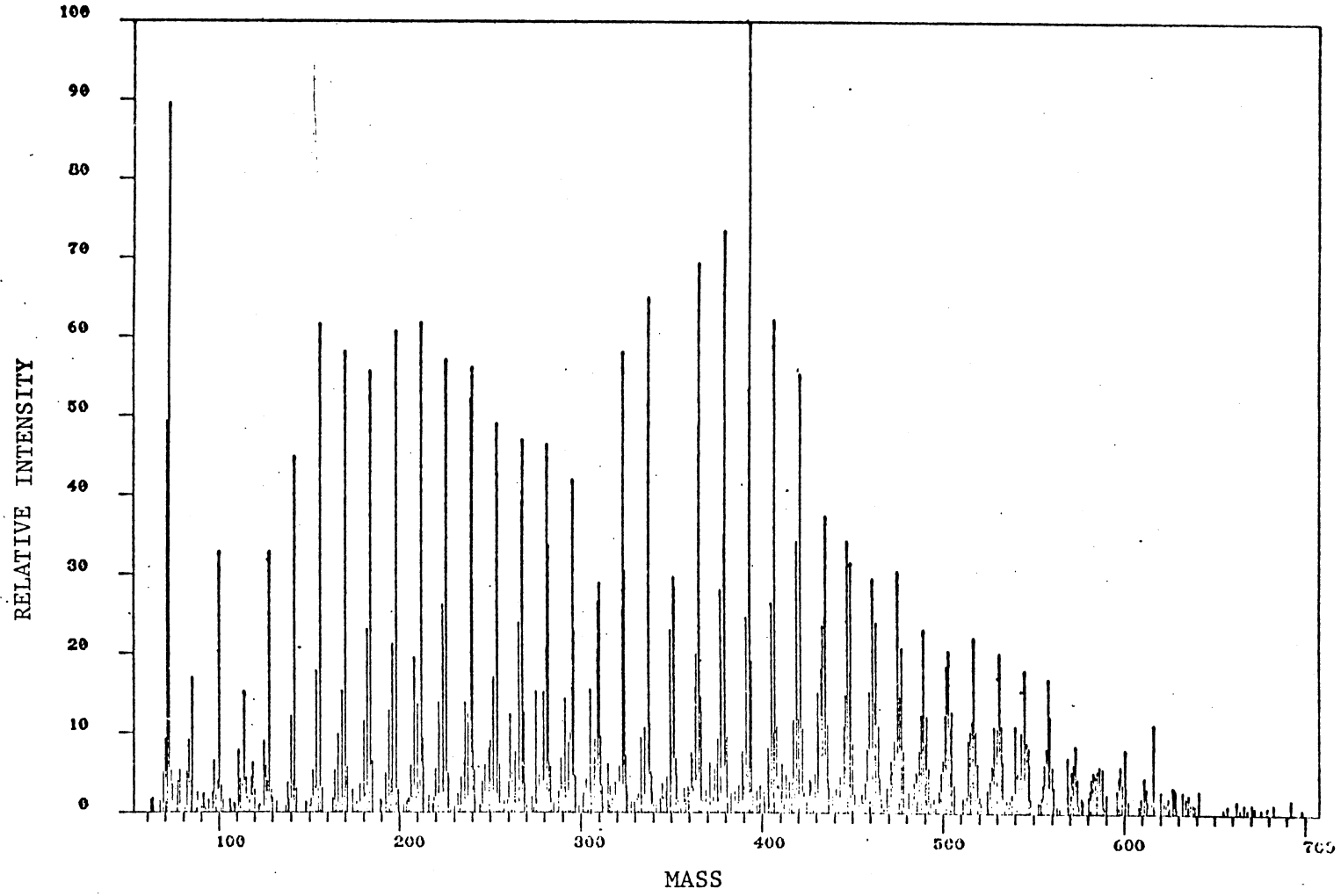

Figure 12. Field Ionization Mass Spectra of Petroleum Saturate Fraction 72054

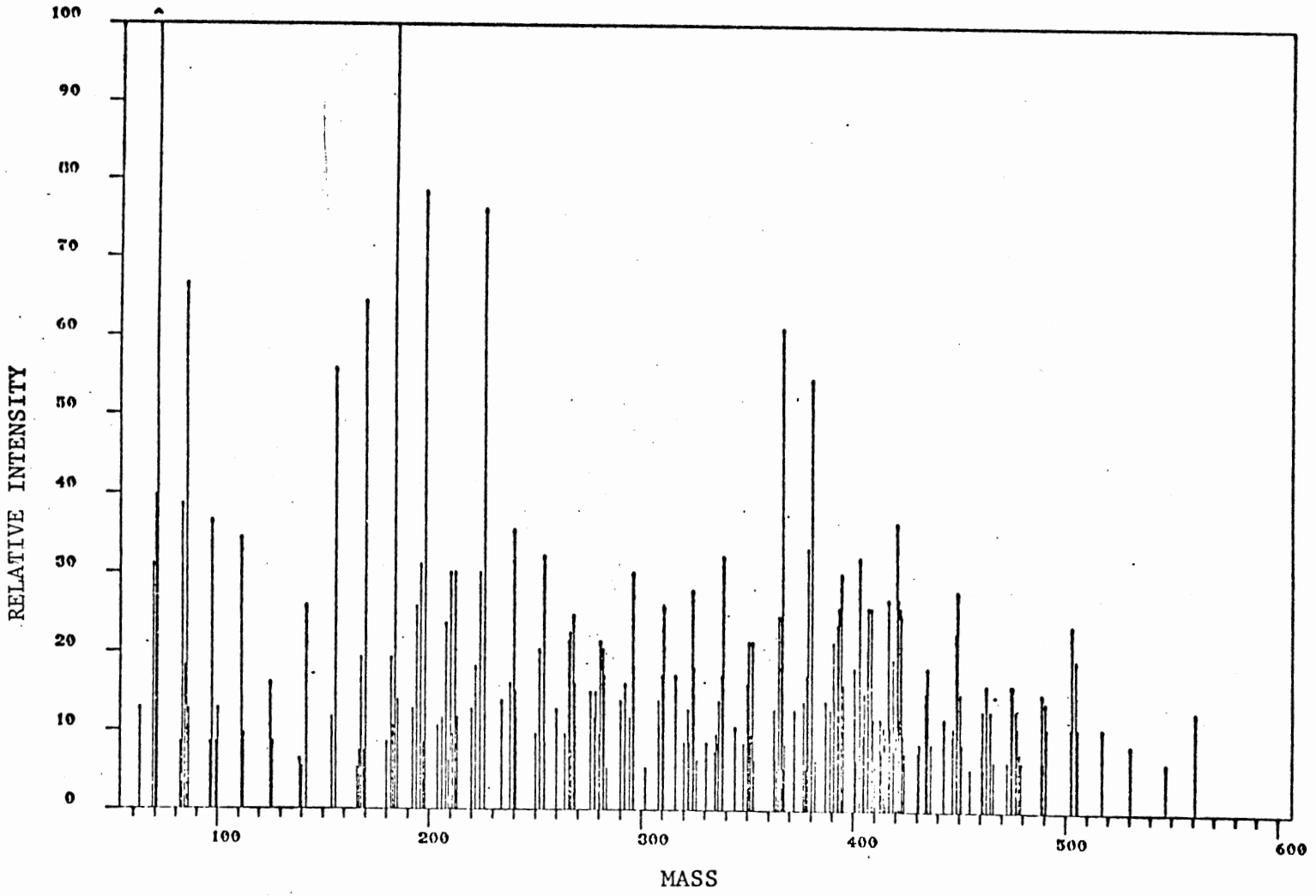

Figure 13. Field Ionization Mass Spectra of Petroleum Saturate Fraction 73065

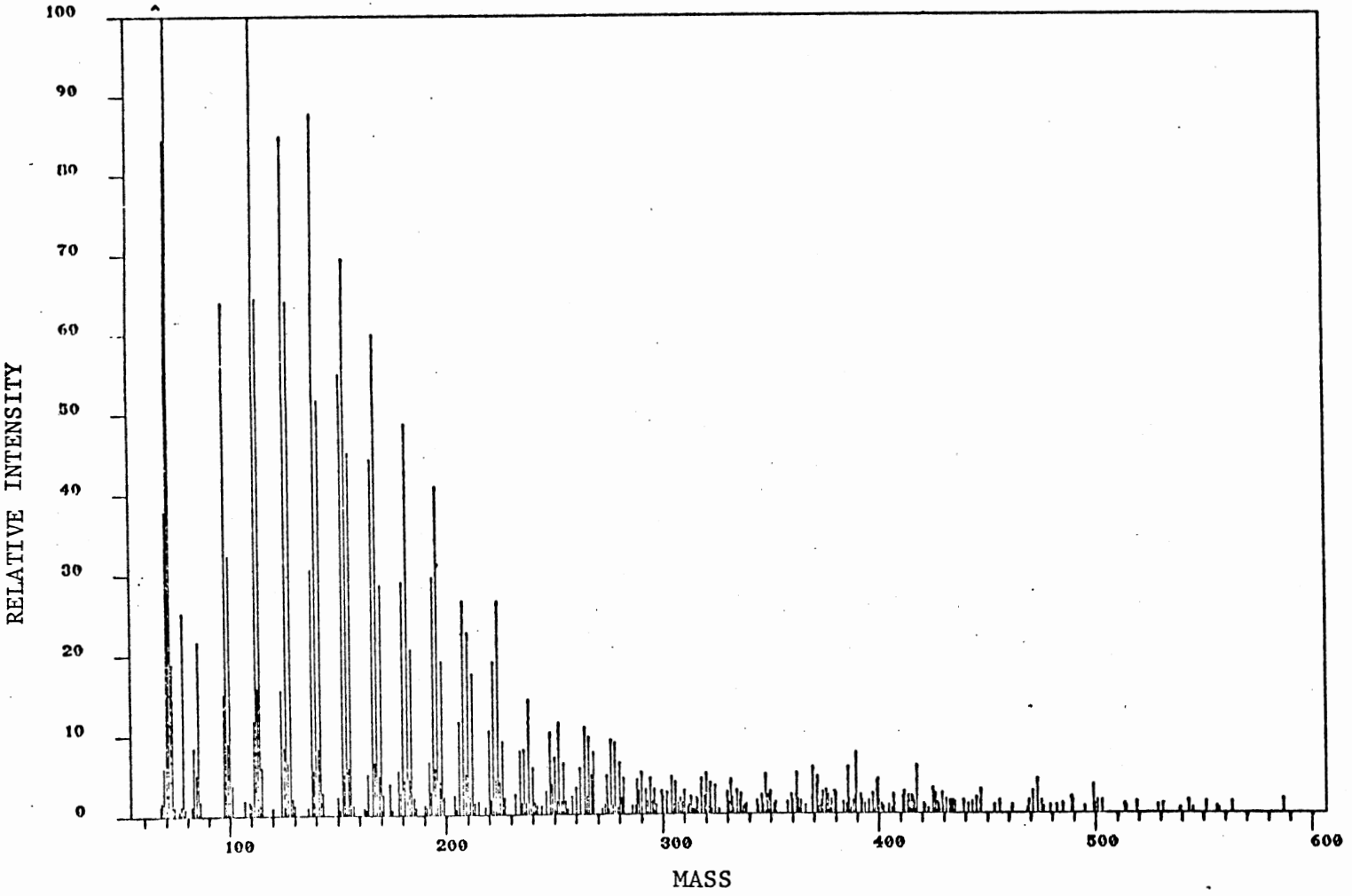

Figure 14. Field Ionization Mass Spectra of Petroleum Saturate Fraction 75046

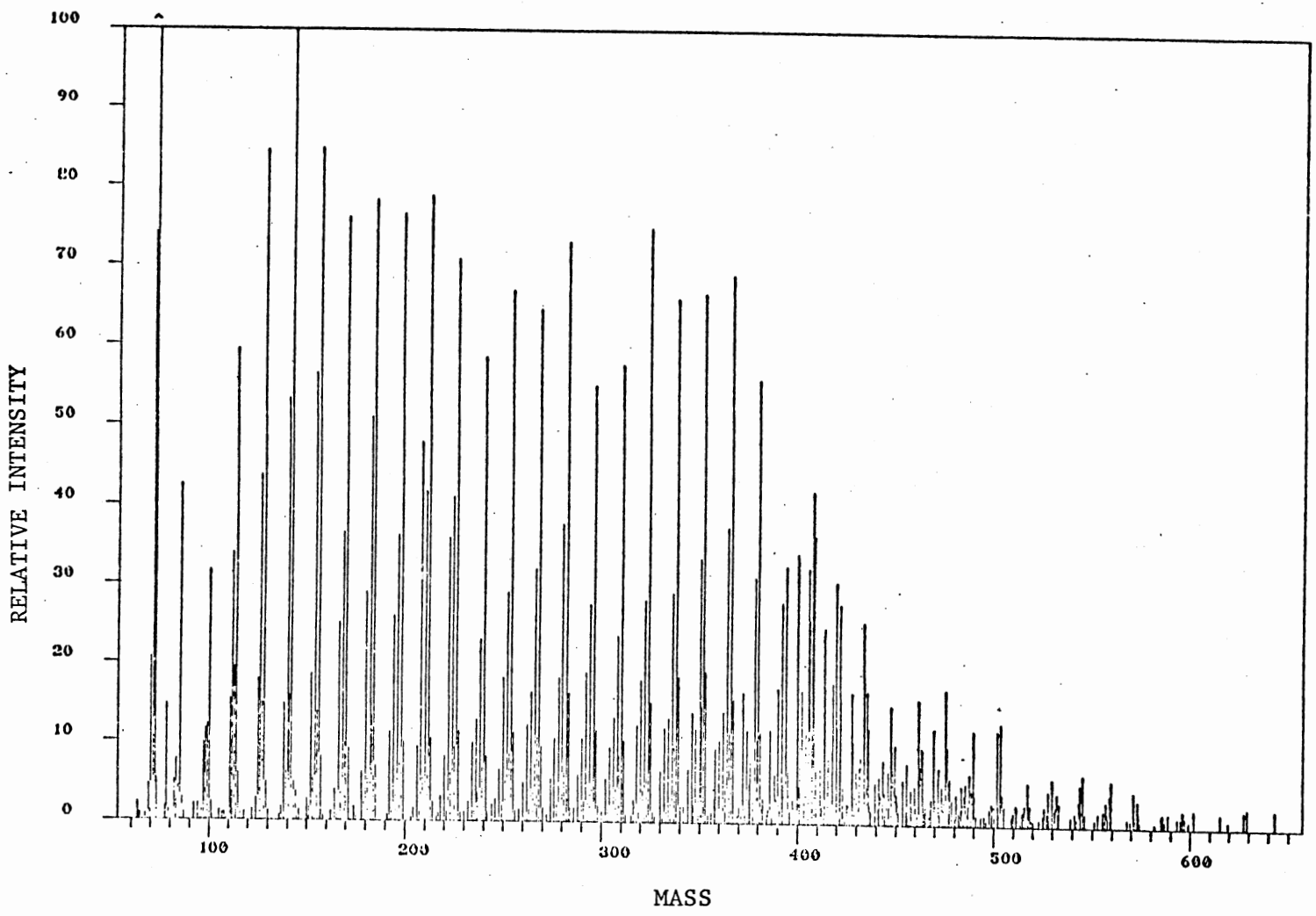

Figure 15. Field Ionization Mass Spectra of Petroleum Saturate Fraction 75052 #1

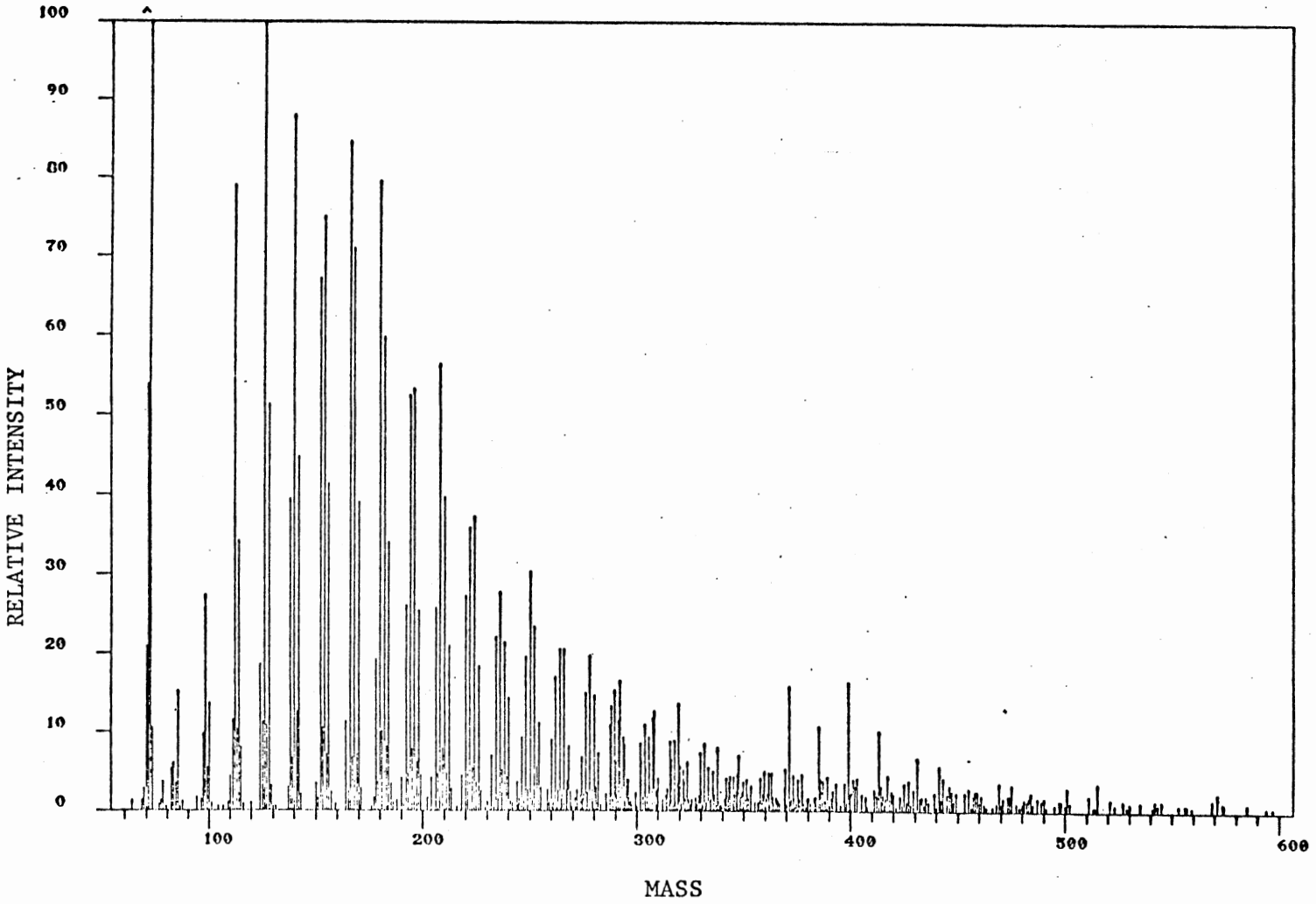

Figure 16. Field Ionization Mass Spectra of Petroleum Saturate Fraction 75052 #2

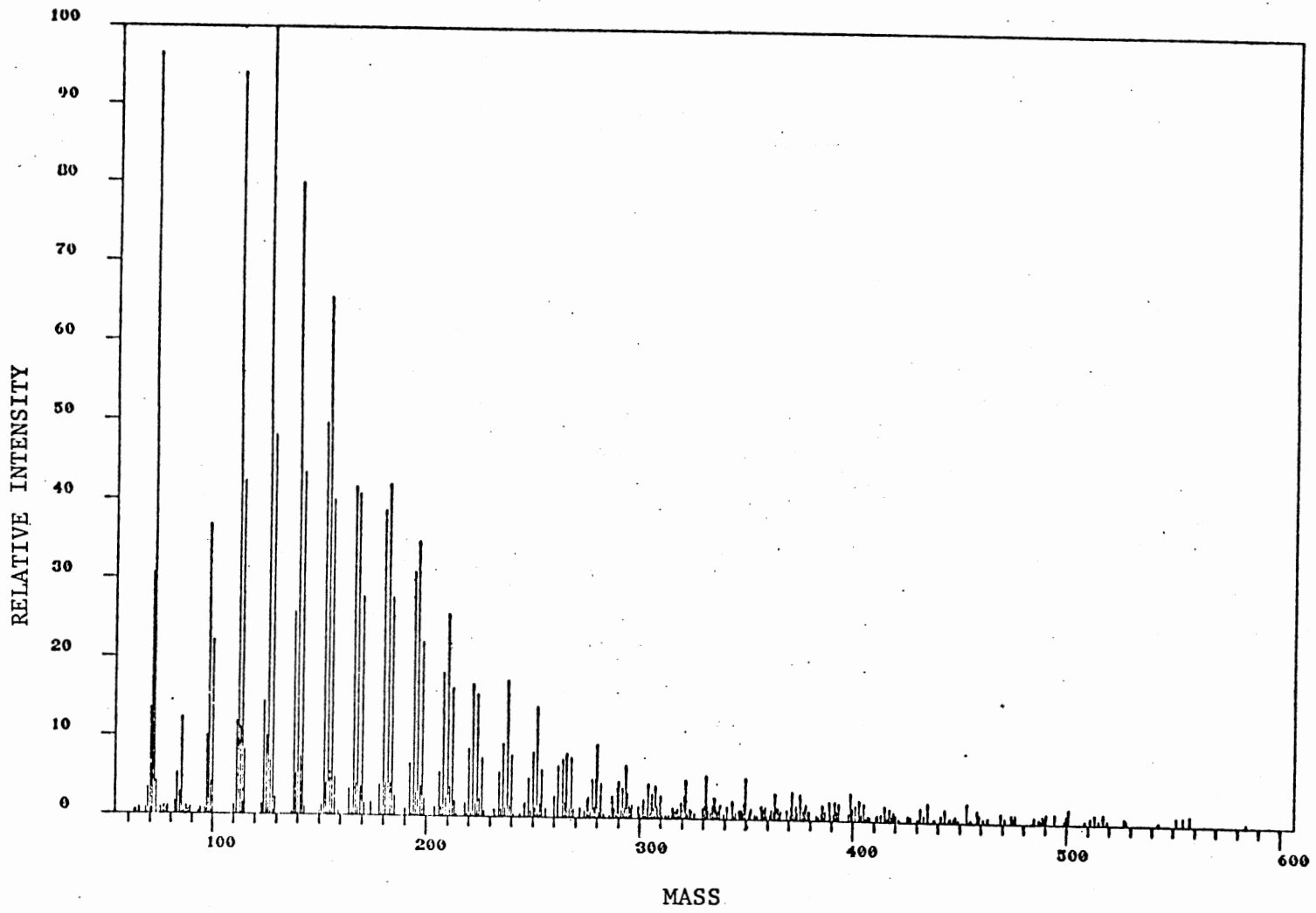

Figure 17. Field Ionization Mass Spectra of Petroleum Saturate Fraction 75064

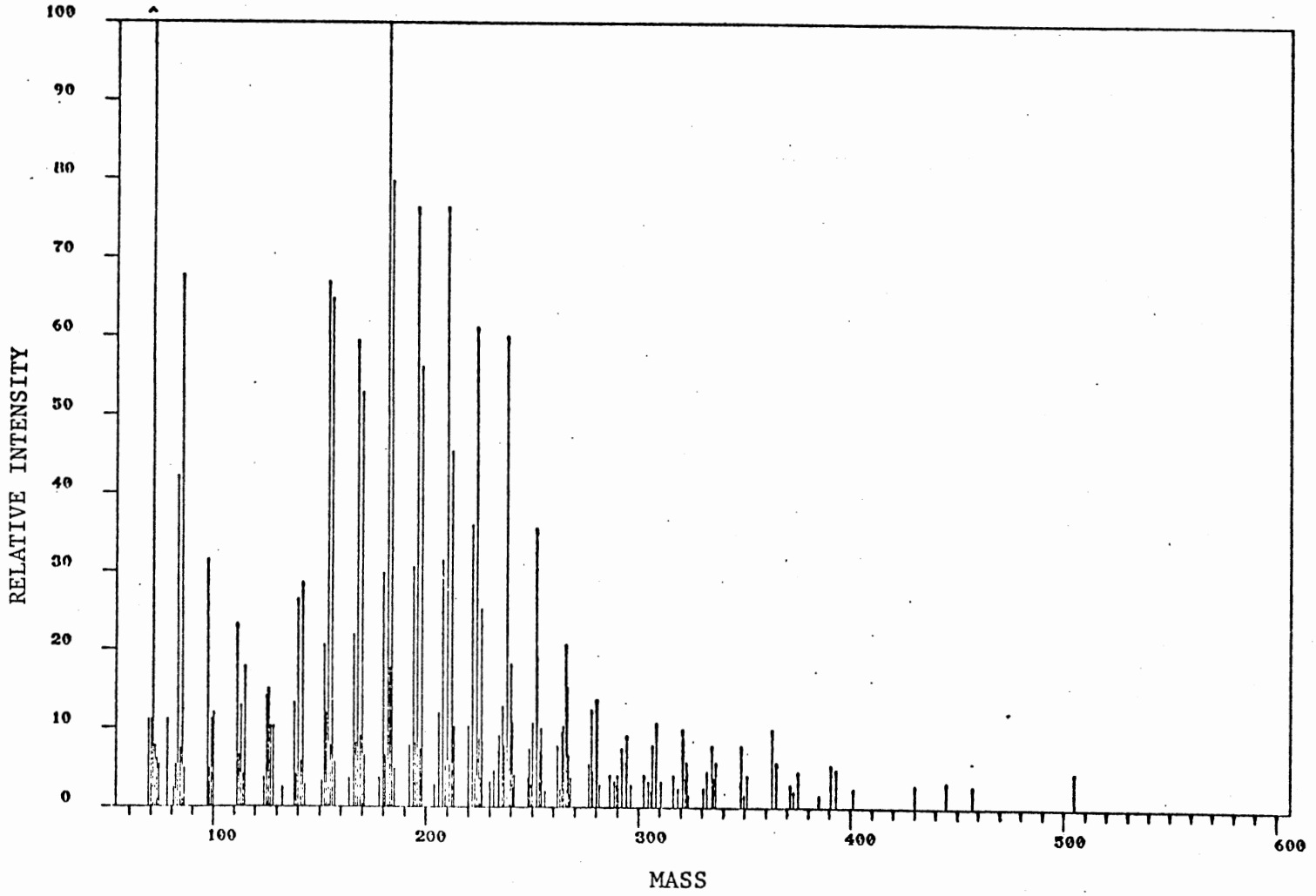

Figure 18. Field Ionization Mass Spectra of Petroleum Saturate Fraction 76046

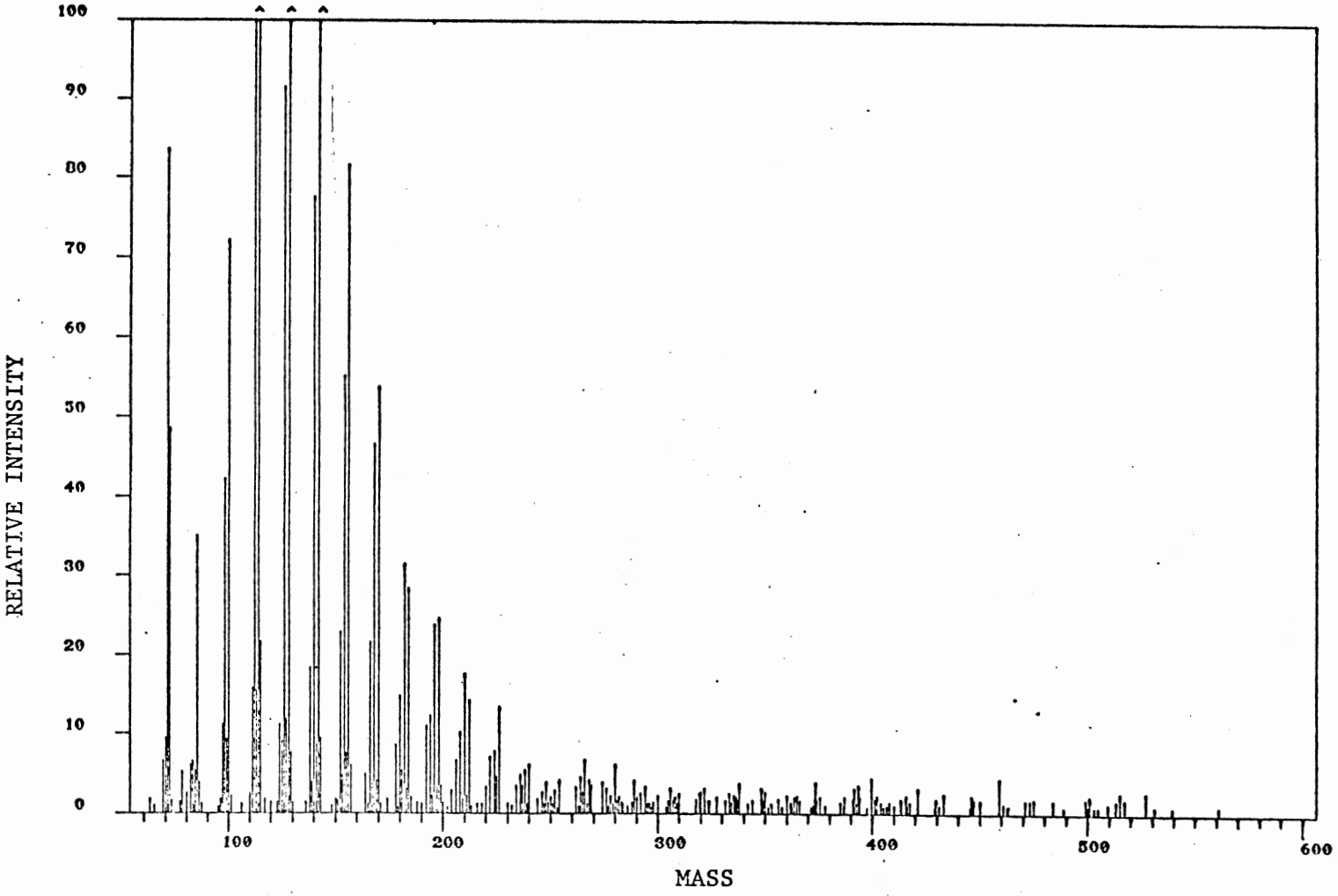

Figure 19. Field Ionization Mass Spectra of Petroleum Saturate Fraction 78001

TABLE XXIII

CHARACTERIZATION OF PETROLEUM SATURATE FRACTIONS BY TOTAL SAMPLE CARBON NUMBER DISTRIBUTIONS

Sample Number	Run Number	Carbon Number			
		Maxima	Weight % of Maxima	Range	Average
71011	1	9	10.18	6-40	12.61
	2	11	11.65	6-41	12.63
72054	1	14	4.09	6-46	19.24
	2	12	9.50	6-43	14.37
73065	1	13	8.69	6-36	17.07
75046	1	8	13.67	6-37	11.12
	2	10	12.53	6-38	11.51
75052F1	1	10	5.77	6-42	16.05
	2	8	13.04	6-36	11.21
75052F2	1	9	11.69	6-33	12.12
	2	10	13.29	6-35	10.76
75064	1	9	13.81	6-38	11.30
	2	9	15.95	6-39	10.59
76064	1	13	15.55	6-25	13.01
78001	1	8	21.58	6-38	10.15
	2	9	19.41	6-34	10.32

was at m/e 100. The peak on the lower mass side of this doublet was attributed to septum bleed. On the average, the peak due to the septum accounted for 80% of the total ion intensity of m/e 100. This was taken into account in all scans and corrected.

Previously, a saturate fraction of petroleum #72054 was run by field-ionization and 70-eV eletron-impact mass spectrometry in order to check the correlation between the quantitative results of the two methods. The results from this analysis are given in Table XXIV. The quantitative results for the 70-eV spectra were obtained at the Bartlesville Energy Technology Center using standard matrix methods (27). The group type analysis for these two methods compare favorably well. The carbon number distribution varies somewhat from that of the runs in Table XV, since the separation cut point for this fraction was different. However, the weight percent distributions for the homologous series compare very well with the results from Run#2.

In summation, quantitative analysis by field-ionization mass spectrometry of petroleum saturate fractions is feasible for characterization studies. Quantitation is directly dependent on the availability of FI experimental sensitivity coefficient data and the ability to predict further coefficients from the available values.

On the basis of a minimum of two runs, distinguishing trends may be seen in each of the petroleum saturate fraction. Thus, within a ten percent error limit, the resulting analysis of a unknown sample may be compared to the analyzed known samples and may, on the basis of the weight percents of an homologous z-series, carbon number distributions, and average carbon numbers, be found in agreement with some of the known samples, thus elimination of others. With the aid of another analysis

TABLE XXIV

CHARACTERIZATION OF PETROLEUM #72054 SATURATE FRACTION BY FIELD IONIZATION AND 70-EV ELECTRON IMPACT MASS SPECTROMETRY

Z-Series	FI		EI
	Carbon Number Range	Volume Percent	Volume Percent
2	12-33	65.3	70.5
0	12-33	22.4	18.5
-2	13-31	7.5	6.4
-4	14-31	3.4	2.7
-6	19-30	1.0	1.9
-8	27-30	0.4	0.0

technique, such as chromatography, a more specific characterization of an unknown sample would be possible.

A SELECTED BIBLIOGRAPHY

1. E. W. Muller, Z. Physik, 131, 136 (1951).

2. E. W. Muller, Advances in Electronics and Electron Physics, vol.13, Marton, ed., Academic Press, New York, 1960.

3. A. J. Robertson, Field Ionization Mass Spectrometry, Journal of Physics E: Scientific Instruments, vol.7, 1974.

4. H. D. Beckey, H. Knoppel, G. Metzinger, and P. Schulze, Advances in Mass Spectrometry, vol.3, Mead, ed., The Institue of Petroleum, London, 35, 1966.

5. Private communication from S. E. Scheppele.

6. H. D. Beckey, Field Ionization Mass Spectrometry, Pergammon Press, New York, 1971.

7. M. G. Ingram and R. Gomer, J. Chem. Phys., 22, 1279 (1954).

8. R. Gomer, 'Field Emission and Field Ionization', in Harvard Monograph Series in Applied Science, vol.9, Harvard University Press, Cambridge, 1961.

9. J. Block, Advances in Mass Spectrometry, vol.4, Kendrick, ed., Institute of Petroleum, London, 781 (1968).

10. D. F. Brailsford, and A. J. Robertson, Int. J. Mass Spec., Ion Phys., 1, 75 (1963).

11. G. Greenwood, PhD. Thesis, Oklahoma State University, 1977.

12. S. L. Murov, Handbook of Photochemistry, Marcel Dekker, New York, 199 (1963).

13. J. B. Birks, Photophysics of Aromatic Molecules, Wiley, New York, 158 (1970).

14. C. E. Milton and H. W. Joy, Can. J. Chem., 44, 1455 (1966).

15. H. D. Beckey, Ang. Chem.,Int. Ed., 8(9), 623 (1969).

16. Wesson, Tables of Electric Dipole Moments, Tech Press MIT, Boston, 1948.

17. R. J. W. LeFevre, Dipole Moments, 3rd ed., Methuen, London, 1953.

18. S. E. Scheppele, C. S. Hsu, T. D. Marriott, P. A. Benson, K. N. Detwiler, and N. B. Perreira, Int. J. Mass Spectrom Ion Phys., 28, 335 (1978).

19. S. E. Scheppele, P. L. Grizzle, G. J. Greenwood, T. D. Marriott, and N. B. Perreira, Anal. Chem., 48, 2105 (1976).

20. E. A. Moelwyn-Hughes, Physical Chemistry, 2nd ed., Pergammon Press, New York, 1961.

21. J. O. Hirschfelder, C. F. Curtiss, and R. B. Bird, Molecular Theory of Gases and Liquids, Wiley and Sons, New York, 1954.

22. C. G. LeFevre, and R. J. W. LeFevre, Rev. Pure App. Sci., 5(4), 261 (1955).

23. K. G. Denbigh, Trans. Far. Soc.,36, 936 (1940).

24. C. G. LeFevre, and R. J. W. LeFevre, Physical Methods in Organic Chemistry, vol.1, chp.36, Weissberger, ed., International Publishers, New York, 1960.

25. R. D. Grigsby, C. O. Hansen, D. G. Mannering, W. G. Fox, and R. H. Cole, Anal. Chem. 43, 1135 (1971).

26. S. D. Christian, J. Chem. Ed., 42, 604 (1965).

27. Annual Book of ASTM Standards, Petroleum Products and Lubricants, II, 24, 700 (1977).

APPENDIX A

CALCULATION OF POLARIZABILITIES

In electrostatic induction, the term polarization refers to the displacement of charges that occur in a substance when it is placed in an electric field (20,21). The polarization which results from a displacement of electron clouds relative to atomic nuclei is termed electronic polarization. For molecular substances, polarization may occur as a consequence of the distortion of the molecular skeleton. Together, these two kinds of polarization are called distortion polarization. Finally, for molecules which possess permanent dipole moments, the application of a electric field produces a small preferential orientation of the molecular dipoles in the direction of the field. The magnitude of the average induced dipole is proportional to the field strength (F). Thus, the mean moment may be expressed as,

$$\mu = \alpha F \tag{33}$$

The polarizabiltiy of a body is mathematically described in equation 34 by an ellipsoid of polarizability possessing three orthogonal semi-axes, b_1, b_2, and b_3 (22). The points represented by the coordinates x, y, and z lie on a surface which in turn may be viewed as containing the imaginary end points of moment vectors induced when a unit

$$\frac{x^2}{b_1^2} + \frac{y^2}{b_2^2} + \frac{z^2}{b_3^2} = 1 \tag{34}$$

field is successively applied to the molecule in all possible orientations. In the case where the external field acts at an angle to b_1, b_2, or b_3, the induced moment will lie at an angle to the field direction. Thus, the magnitude of the polarizabilities depend on the orientations of the molecules in the field, i.e., the field induces component moments parallel to itself. Only when the field is parallel to one of the semi-axes, b_1, b_2, or b_3, will such perpendicular components be zero; the moments induced in these special cases are known as the principle polarizabilities, b_1, b_2, and b_3, of the molecule (see Figure 20). From these principle polarizabilities, the mean molecular polarizability may then be defined as equation 35.

$$\alpha = 1/3(b_1 + b_2 + b_3) \tag{35}$$

Landolts rule (23) states, to a first approximation, that the molar polarizability of a component is the sum of the atomic polarizabilities of its constituents. Perfect additivity, however, could only occur if all the atoms in the molecule were entirely without effect on each other, i.e. no bond formation. A simple improvement on Landolt's rule is to assume that there is an additivity of bond polarizabilities (23). Such bond polarizabilities have been calculated by LeFevre (22, 24) from measurements of the Kerr effect and are given in TABLE XXV.

From these bond polarizabilities, summations of terms yield the mean polarizabilities which may then be used for the determination of the supply function. Hexane is a simple example for illustration of the additivity of mean bond polarizabilities.

$$\begin{aligned} 5(C\text{-}C) &= 5(0.51) = 2.55 \\ 14(C\text{-}H) &= 14(0.64) = \underline{8.96} \\ & \qquad\qquad 11.51 \ \text{Å}^3 \end{aligned}$$

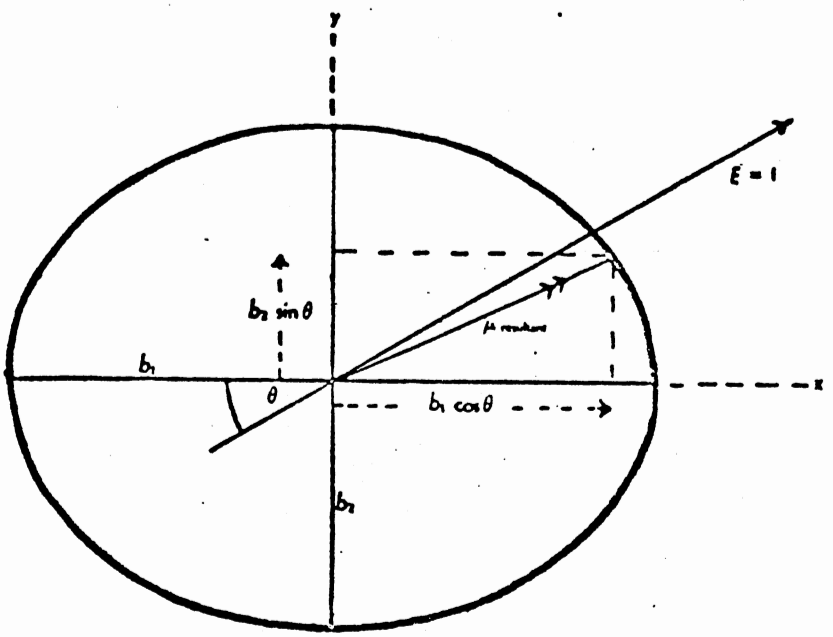

Figure 20. Polarizability Ellipsoid With Semi-axes b_1, and b_2

TABLE XXV

PRINCIPLE AND MEAN BOND POLARIZABILITIES

Bond	Polarizabilities ($\AA^3$)			
	b_1	b_2	b_3	α
C-C (aliphatic)	0.99	0.27	0.27	0.51
C-C (aromatic)	2.24	0.21	0.59	1.01
C-H	0.64	0.64	0.64	0.64
C=C	2.80	0.73	0.77	1.43
C≡C	3.50	1.30	1.30	2.03
C=O	2.30	1.40	0.46	1.39
C-O	0.81	0.46	0.46	0.53
O-H	1.80	2.00	1.66	1.82
C-N	0.57	0.69	0.69	0.65
N-H	0.50	0.83	0.83	0.72
C-Cl	3.90	1.85	1.85	2.53
C-Br	5.40	2.70	2.70	3.60

APPENDIX B

MICROMOLECULAR PROBE DISTILLATION

Micromolecular probe distillation, a term coined by Grigsby (24), in mass spectrometric analysis refers to the controlled temperature distillation of a very small amount of sample from a direct insertion probe into the ion source. Micromolecular distillation data are obtained by distilling a sample placed in a glass probe at a constant rate of temperature increase, usually 5^{o}/min. During the distillation, multiple mass spectra and temperature data are taken. An online data acquisition routine reduces the raw data, stores the resulting peak intensity and time centroid in a time file and stores the probe-temperature data in an auxiliary file. The offline data acquisition routine assigns the m/e values to the peaks according to their time centroid values, then stores the m/e values and peak intensities in a mass file. All peaks are then assigned a temperature from the time centroid and probe temperature data.

The peak intensity/temperature pairs along with their associated m/e values may be plotted to give an elimination curve, similar to those obtained for macro scale distillation. The data are handled by a computer program which uses a least squares technique to fit the points to an emperical equation (25).

$$INT(CALC) = \frac{A \exp(-B/T_i)}{1 + \exp\ C(T_i - D)} \qquad (36)$$

where T_i is the absolute temperature at point i and A, B, C, and D are

parameters evaluated from the least squares fit.

Once, the parameters A, B, C, and D are evaluated, three quantities of importance are obtained from the computer output. These are:

1) $T(I_m)$ - the temperature at curve maxima,

2) I_m - the maximum intensity of the curve, and

3) Area - the area under the curve.

Thus, the relative gram sensitivities for components of a mixture of known composition may be obtained by equation (37).

$$Sg_i = \frac{(Area_i)(gm_R)}{(Area_R)(gm_i)} \tag{37}$$

The results obtained from the FI/MS analysis of the distillation of the n-paraffin mixtures are representative of the data presented in Tables XXVI and XXVII, and Figures 21 and 22. Columns 1 and 2 of Tables XXVI and XXVII contain temperatures and corresponding FI/MS intensities for the molecular ions at masses 254 and 268, respectively. Column 3 in each Table contains the intensities calculated from a least squares fit of the experimental molecular-ion intensities to temperature. The data in Tables XXVI and XXVII are plotted in Figures 21 and 22, respectively. The elimination curves for the distillation/ionization of octadecane and nonadecane fit the experimental intensities quite well.

TABLE XXVI

EXPERIMENTAL AND CALCULATED DEPENDENCE OF THE FI/MS ION ABUNDANCE AT M/E 254 ON TEMPERATURE AND PARAMETERS USED IN AND OBTAINED FROM CONSTRUCTION OF ELIMINATION CURVES

PRSM1 M/E 254.0

TEMP	INT(EXP)	INT(CALC)
313.	198.	97.
320.	157.	174.
326.	275.	279.
332.	464.	434.
336.	521.	566.
340.	788.	707.
345.	810.	836.
350.	790.	809.
356.	581.	566.
362.	298.	305.

T1 = 326. I1 = 275. T2 = 340. I2 = 788. T3 = 350. I3 = 790. T4 = 362. I4 = 298.

A = 0.365E+14 +-0.2E+13 B = 0.8342E+04 +-0.2E+02 C = 0.20E+00 +-0.3E-01 D = 0.3500E +-0.1E+01

SIGMA = 0.595E+02 NUMBER OF ITERATIONS = 4

T(IMAX) = 0.3469E+03 +-0.143E+01 IMAX = 0.8489E+03 +-0.116E+03 AREA = 0.2377E+05 +-0.307E+04

TABLE XXVII

EXPERIMENTAL AND CALCULATED DEPENDENCE OF THE FI/MS ION ABUNDANCE AT M/E 268 ON TEMPERATURE AND PARAMETERS USED IN AND OBTAINED FROM CONSTRUCTION OF ELIMINATION CURVES

PRSM1 M/E 268.0

TEMP	INT(EXP)	INT(CALC)
313.	76.	46.
320.	35.	78.
326.	142.	123.
331.	150.	176.
336.	236.	250.
341.	495.	350.
345.	414.	456.
350.	722.	629.
356.	813.	890.
362.	701.	677.
368.	45.	59.

T1 = 326. I1 = 142. T2 = 350. I2 = 722. T3 = 356. I3 = 813. T4 = 362. I4 = 701.

A = 0.283E+13 +-0.3E+12 B = 0.7779E+04 +-0.4E+02 C = 0.58E+00 +-0.4E+00 D = 0.3621E+03 +-0.9E+09

SIGMA = 0.775E+02 NUMBER OF ITERATIONS = 6

T(IMAX) = 0.3584E+03 +-0.151E+01 IMAX = 0.9496E+03 +-0.209E+03 AREA = 0.2023E+05 +-0.313E+04

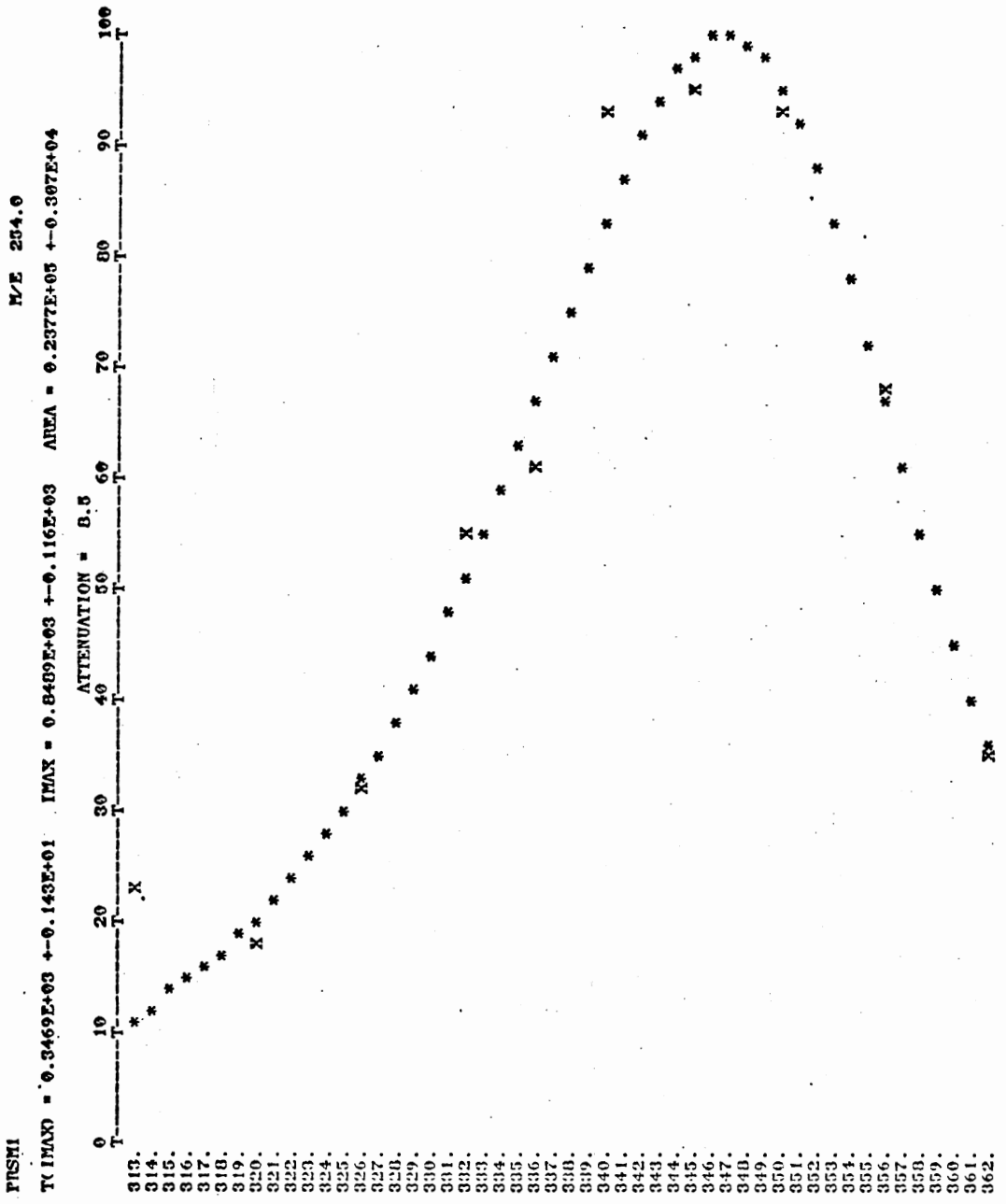

Figure 21. Elimination Curve for Distillation of n-Octadecane. Points Designated by x and * Correspond to Attentuated Relative Abundances for m/e 254 as a Function of Probe Temperature (^{o}K)

Figure 21. Elimination Curve for Distillation of n-Octadecane. Points Designated by x and * Correspond to Attenuated Relative Abundances for m/e 254 as a Function of Probe Temperature (^{o}K).

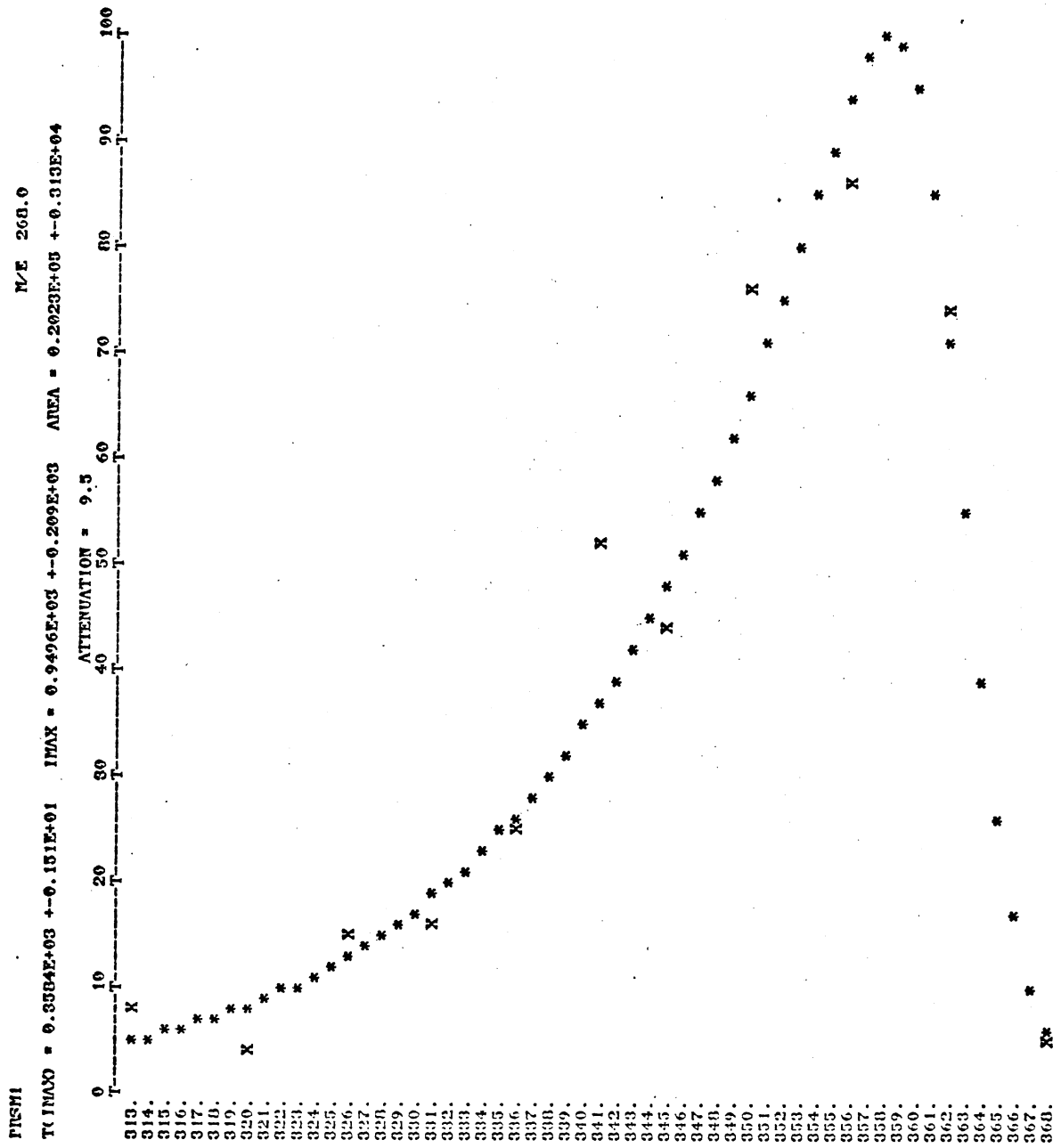

Figure 22. Elimination Curve for Distillation of n-Nonadecane. Points Designated by x and * Correspond to Attenuated Relative Abundances for m/e 268 as a Function of Probe Temperature (^{o}K)

Figure 22. Elimination Curve for Distillation of n-Nonadecane. Points Designated by x and * Correspond to Attenuated Relative Abundances for m/e 268 as a Function of Probe Temperature (^{o}K).

VITA[2]

Michele Rae Derrick

Candidate for the Degree of

Master of Science

Thesis: DETERMINATION OF FIELD IONIZATION SENSITIVITY COEFFICIENTS AND CHARACTERIZATION OF PETROLEUM SATURATE FRACTIONS BY MASS SPECTROMETRY

Major Field: Chemistry

Biographical:

Personal Data: Born in Enid, Oklahoma, March 1, 1955, the daughter of Mr. and Mrs. John Derrick.

Education: Graduated from Enid High School, Enid, Oklahoma, in May, 1973; received Bachelor of Science degree in Chemistry from Central State University, Edmond, Oklahoma, in May 1977; completed requirements for the Master of Science degree at Oklahoma State University, Stillwater, Oklahoma, in December, 1979.

Professional Experience: Student Chemist, Phillips Petroleum Company, summer 1976; Microscopist, Phillips Petroleum Company, summer 1977; Graduate Research Assistant, Oklahoma State University, 1977-1979.